

Waveforms for Computing Over the Air

Ana Perez-Neira^{*†}, Marc Martinez-Gost^{*}, Alphan Şahin[‡],

Saeed Razavikia[§], Carlo Fischione[§], Kaibin Huang[¶]

^{*}Centre Tecnològic de Telecomunicacions de Catalunya, Spain

[†]Dept. of Signal Theory and Communications, Universitat Politècnica de Catalunya, Spain

[‡]Dept. of Electrical Engineering, University of South Carolina, United States

[§]Dept. of Network and Systems Engineering, KTH University, Sweden

[¶]Dept. of Electrical Engineering, University of Hong Kong, Hong Kong

Emails: {aperez, mmartinez}@cttc.es, asahin@mailbox.sc.edu

{sraz, carlofi}@kth.se, huangkb@eee.hku.hk

ABSTRACT

Over-the-air computation (AirComp) leverages the signal-superposition characteristic of wireless multiple access channels to perform mathematical computations. Initially introduced to enhance communication reliability in interference channels and wireless sensor networks, AirComp has more recently found applications in task-oriented communications, namely, for wireless distributed learning and in wireless control systems. Its adoption aims to address latency challenges arising from an increased number of edge devices or Internet of Things (IoT) devices accessing the constrained wireless spectrum. This paper focuses on the physical layer of these systems, specifically on the waveform and the signal processing aspects at the transmitter and receiver to meet the challenges that AirComp presents within the different contexts and use cases.

I. INTRODUCTION

Over-the-air computation (AirComp) leverages the waveform superposition property of the wireless channel to compute mathematical nomographic functions [1] using data from multiple devices. Unlike the conventional transmit-then-compute approach, AirComp uses signal superposition in the coherent multiple access channel (MAC) to significantly reduce communication resources such as bandwidth and time. With AirComp, the receiver is not interested in the individual transmitted signals, but in their sum, allowing K signals to be sent simultaneously without requiring K orthogonal radio resources. This means, for instance, that if there are $K = 100$ signals of 1s duration each, the K transmissions can be completed in 1s instead of 100s.

Initially considered for wireless sensor networks (WSN), AirComp was disruptive because uncoded transmission, specifically analog amplitude modulation where scaled versions of observations are sent, was proven to be optimal under certain channel models [2]. This approach leverages the structural alignment between the channel and the sufficient statistic for estimating the source (i.e., the sum of the transmissions). Traditional separate source-channel strategies, which encode observations into bits, become suboptimal, making it unnecessary for nodes to encode bits [3]. Intuitively, with a separate source-channel strategy, the sensor measurements are first quantized and encoded into bits, which leads to a logarithmic dependency of the mean squared error (MSE) with respect to the number of sensors K due to the quantization noise; that is $\text{MSE} \geq 1/\log_2(K)$. On the other hand, if the measurements follow uncoded transmissions, this logarithmic dependency disappears and $\text{MSE} \geq 1/K$, resulting in a lower distortion bound. In other words, the transmission of bits does not match the additive structure of the physical wireless channel. Note also that the traditional source-channel separation theorem is not optimal for networked systems with multiple transmitters and/or receivers, such as the MAC, which is the focus of this paper.

Going further, due to the vast amounts of data that the current sensor networks generate, artificial intelligence (AI) has emerged as a framework with new tools to uncover complex relationships among the data and has broadened the spectrum of wireless applications that require some sort of computing beyond simple data fusion. In the current literature, this is commonly known as task-oriented applications [4], which will be of paramount importance in sixth generation (6G) wireless networks. Not only communication but also computing will be key elements; thus indicating a paradigm shift. Future communication systems will prioritize enabling higher-level tasks over merely transmitting data, requiring redesign to meet specific application needs. Reducing computational complexity and delays can be more important than minimizing the bit error rate (BER). Edge learning or distributed machine learning are examples of this transition [5], where due to the substantial number of devices simultaneously transmitting, and their individual huge volume of data, the traditional wireless protocols will lack efficiency. The reason is that they are oblivious to the ultimate tasks, necessitating the development of innovative wireless communication methods, such as AirComp. Wireless data networks, wireless control systems, distributed localization, and wireless system-on-chip are several other notable applications where AirComp can be leveraged to improve spectrum efficiency while reducing latency.

AirComp is a disruptive multiple-access paradigm shift from compute after communicate to compute when communicate. To the authors' knowledge, in the literature on AirComp (see [5], [6], [7] as interesting overview papers), there is no work that discusses in detail the basics of the underlying signal processing methods at the transmitter and receiver for computation and waveform generation, and how they address the challenges in practical multiple access channels to achieve a successful transmission. Namely, most

of the existing works assume ideally aggregated signals at baseband, without paying attention to the required transmitted waveform or modulation to achieve this ideal model. Specifically, multipath fading, imperfect power control, and synchronization errors [8] can complicate or even invalidate the design of a reliable AirComp scheme, where the receiver (e.g., fusion center) does not have access to the individual transmitted signals. *How can multi-access be designed to ensure the most efficient collection of the transmitted data by a fusion center?* In this paper, we revisit the waveforms and the signal processing that can be used in order to jointly design the physical layer and multi-access wireless channel for the purpose of function computation. Both perfect and imperfect channel state knowledge are considered. We highlight the existence of many research gaps that have to be resolved in the field of signal processing, to bring AirComp to a practical implementation. Currently, these facts have been noticed by various authors under different perspectives and papers are proliferating in waveform design; thus, motivating this paper to present a systematic introduction of the fundamental signal processing techniques and guidelines to solve the physical layer for AirComp. It is a well-defined, re-emerging area, and reasonably matured in some aspects, that deserves attention by the signal processing community as AirComp opens new avenues for the researchers.

This paper is structured as follows: Section II states the signal processing problem of computing functions over multiple access channels, with a brief discussion on applications and metrics; Section III and IV overview analog and digital modulations for AirComp, respectively; The physical layer frame, which confers diversity and multiplexing capabilities to the system, is presented in Section V. Next, the signal processing techniques that can be implemented in this physical frame depending on the available channel state information are presented in Section VI. Section VII comments on the security concerns of AirComp, and Section VIII concludes the paper and proposes future research directions.

II. COMPUTING FUNCTIONS OVER MULTIPLE ACCESS CHANNELS

A. Applications

In the era of big data, the interest in developing AirComp schemes stems from the vast number of applications that require computing a function of distributed data. In that case, AirComp can be exploited to reduce the communication bottlenecks (e.g., delay, bandwidth and power), as well as the computational burden at the receiver side or end device. Consequently, AirComp can be part of the efficient execution of these computations, and this paper reviews how to compute diverse functions beyond the classic sum or averaging.

The most notorious current application of AirComp is federated edge learning (FEEL) [5], in which the nodes train a shared model collaboratively by exchanging model parameters or gradients with a

fusion center, e.g., an access point or a base station. By means of AirComp, all nodes can transmit each model parameter simultaneously and the receiver obtains a statistical average (e.g., arithmetic mean, median) of the models. The aggregated parameters are then distributed back to the devices for further updates until convergence. Another application is MapReduce [9]. The intuition behind MapReduce is that many functions computed over large datasets can be decomposed into sub-tasks that can be processed in parallel and distributed fashion. In the context of data centers, [10] proposes to resolve data erasures using network-coded storage. Particularly, a weighted sum of the distributed data is used as a key to recover the data of a specific node.

Wireless sensor networks and control systems are other areas where AirComp can be utilized for information gathering. In [11], different cameras track a target to implement a distributed Kalman-consensus filter. The sum of the different estimates between neighboring cameras is achieved with AirComp. In [12], the max-pooling operation of a distributed neural network is implemented with AirComp. In [13], the distance among cars in a vehicle platoon is controlled with an AirComp policy, in which the statistical information (e.g., maximum and minimum data), may be critical. Moreover, many standard signal processing techniques (e.g., singular-value decomposition, k -means, independent component analysis) can be expressed as weighted sums. In [14], AirComp is considered for the federated k -means clustering algorithm.

Furthermore, lately it is gaining momentum to interconnect a large number of physically distributed in-memory computing cores. This is the case of hyperdimensional computing (HDC), which can benefit from the concurrent transmission that AirComp enables [15].

B. Problem Statement

Consider a multiple access network comprising K distributed nodes that operate as data sources or transmitters, and a single node at the receiver side, which we refer to as receiver or fusion center. The ultimate goal of the network is to perform data fusion at the receiver side, this is, to compute a function that conveys information from the distributed data. The transmitting nodes may be sensors, in which the data corresponds to measurement readouts, or computing nodes, where the associated data originates from a local computation. In this formulation, the network consists of a MAC with certain peculiarities in its application and usefulness, which is known as AirComp, as it will be described in the following.

Each node has a readout $s_k \in \mathbb{E} \triangleq [0, 1] \in \mathbb{R}$, which we consider stays fixed during a period of time T . The network computes a function defined as $f(s_1, \dots, s_K) : \mathbb{E}^K \rightarrow \mathbb{R}$. We particularly constrain the functions of interest to be symmetric, i.e., any permutation of the arguments of the function does not change the function output. Thus, only the data is relevant, not the origin nodes. For instance, arithmetic

mean, maximum, and majority voting are several symmetric functions among many other statistical functions. Note that the source of the readings may be a computer or perhaps a natural phenomenon in the case of sensor nodes. Therefore, to keep the explanation general enough, we will not go into the model between the information source and the transmitting node. This is in contrast to other seminal works, such as [16], which deals solely with sensor networks and focuses on the channel between the source and the node.

The signals of all K transmitting nodes are sent simultaneously, thus not necessarily consuming different radio resources. In this way, the additive nature of the MAC can be exploited to compute the desired function f as explained next. At this stage, we consider a baseband model and several orthogonal radio resources $l = 1, \dots, L$ (i.e., time, frequency, or code), enabling the application of AirComp to angular modulated signals, among other functionalities. Given a set of K readouts, s_k , the signal at the input of the receiver at the resource l is

$$y_l = \sum_{k=1}^K h_{kl} \varphi_{kl}(s_k) + w_l, \quad (1)$$

where h_{kl} is the channel coefficient between the sensor k and the fusion center in the radio resource l ; φ_{kl} is the transmitted signal by the node k , which depends on the node data k and acts on the same value s_k for all l , and w_l is the receiver noise. Perfect synchronization among the K transmitters is assumed. Equation (1) is a high-level model abstraction that helps to introduce the problem. Later, this article will complete and detail (1) by introducing the modulations and processing that will allow its interpretation and implementation.

In the case of an ideal coherent MAC, i.e., without fading channel and noise at the receiver, (1) reduces to

$$y_l = \sum_{k=1}^K \varphi_{kl}(s_k), \quad (2)$$

which highlights the additive nature of the wireless MAC. The aim is to harness co-channel interference to compute a linear combination of functions of the measurements. For this reason, there is no need for the receiver to recover each signal separately. An immediate consequence of this approach is a higher computation throughput, and, with it, a reduced latency or lower bandwidth requirements. For instance, to compute the arithmetic mean in an ideal MAC, each transmitter transmits $\varphi_{kl} = s_k/K$ (assuming that the number of nodes in the computation is known at the transmitter), and the function is just the received symbol, i.e., $f = y_l$. In this case, notice that a single radio resource is sufficient to compute f , instead of L .

The information-theoretic result of [2] suggests that the superposition property of the wireless channel

can be beneficially exploited if the MAC is matched in some mathematical sense to the function being computed. The approach is known as computation over the air (so-called AirComp in the present work). Next, we generalize the model in (2) as

$$\psi_l(y_l) = \psi_l \left(\sum_{k=1}^K \varphi_{kl}(s_k) \right), \quad (3)$$

where φ_{kl} and ψ_l are called the pre- and post-processing functions, respectively. Notice that both functions depend on the radio resource l . Encompassing pre-processing and post-processing functions, the additive MAC is transformed into an equivalent channel that aims to match the structure of the function to be computed. Finally, the function of interest is obtained by appropriately combining the post-processed measurements with a function Ψ :

$$f(s_1, \dots, s_K) = \Psi(\psi_1(y_1), \dots, \psi_L(y_L)) . \quad (4)$$

The multivariate functions that can be represented as in (3) are called *nomographic* and are the fundamental building block for AirComp systems [17]. While this representation stems from an analytical function representation, researchers in the fields of signal processing and communications have noticed that such representation can be used for distributed computations: 1) Pre-processing functions can be computed at each transmitter in a distributed fashion, 2) Post-processing functions are computed at the receiver side, and 3) The sum is performed by the MAC. Any function computation approach that exploits the wireless MAC via (3) is called an AirComp scheme.

Going a step further, to describe any continuous and multivariate f , the Kolmogorov-Arnold theorem provides the existence of such representation using universal (i.e., independent of f) continuous pre-processing functions and multiple post-processing functions. Particularly, f can be represented as

$$f(s_1, \dots, s_K) = \sum_{l=1}^{2K+1} \psi_l \left(\sum_{k=1}^K \varphi_{kl}(s_k) \right), \quad (5)$$

where the post-processing functions depend on f and the aggregation function Ψ corresponds to the sum. From the network perspective, having universal pre-processing functions results in having no additional feedback when an alternative function has to be computed. On the other hand, the expression (5) manifests that the network requires $L = 2K + 1$ to compute the function. The theorem proves the existence, not the construction of the corresponding preprocessing and postprocessing functions. It does not identify L with radio resources either. In general, this theorem provides a fundamental guide, and we refer the curious reader to [18], where the authors use a neural network architecture inspired by the Kolmogorov-Arnold

TABLE I
EXAMPLE NOMOGRAPHIC FUNCTIONS [6].

Description	$f(s_1, s_2, \dots, s_K)$	$\varphi_k(x)$	$\psi(x)$
Arithmetic mean	$\frac{1}{K} \sum_{k=1}^K s_k$	x	$\frac{x}{K}$
Majority vote	$\text{sign} \left(\sum_{k=1}^K \text{sign}(s_k) \right)$	$\text{sign}(x)$	$\text{sign}(x)$
p -norm	$\left(\sum_{k=1}^K s_k ^p \right)^{1/p}$	$ x ^p$	$x^{\frac{1}{p}}$
Approximation of the geometric mean	$\left(\prod_k s_k \right)^{1/K}, s_k \geq 0$	$\ln \left(x + \frac{1}{p_0(\epsilon)} \right)$	$e^{\frac{x}{K}}$
Approximation of the maximum	$\max_k \{s_k\}, s_k \geq 0$	$x^{p_0(\epsilon)}$	$x^{\frac{1}{p_0(\epsilon)}}$
Approximation of the minimum	$\min_k \{s_k\}, s_k \geq 0$	$x^{-p_0(\epsilon)}$	$x^{-\frac{1}{p_0(\epsilon)}}$

theorem and propose Fourier series expansions to implement the φ_{kl} . In practice, it may be desirable to reduce the number of radio resources; thus, computing a nomographic approximation, this is, a function that approximates the original f with respect to the precision ϵ :

$$\left\| f - \psi \left(\sum_{k=1}^K \varphi_k(s_k) \right) \right\|_{\infty} \leq \epsilon \quad (6)$$

In AirComp, the approximation is mandatory due to the existence of a communication channel. In this respect, we identify L with radio resources and introduce up to L pre-processing functions per transmitter (note that in 6 $L=1$). Later on in section V we introduce additional Q radio resources to counteract the channel impairments, such as noise or interference. They will be independent of the L communication resources associated to pre-processing functions required to approximate f .

Table I displays the pre- and post-processing functions to compute a variety of nomographic functions. Notice that in some cases, the decomposition is exact, while in other cases, it is just an approximation according to (6). In this respect, throughout the rest of the paper, we consider a computation of a single function f . Fig. 1 shows the system diagram to implement an AirComp scheme over a MAC channel. The AirComp modulation (MOD) and demodulation (DEMODO) blocks are explicitly shown in the diagram. As discussed previously, while we assume a single pre-processing function $\varphi_k(s_k)$ per transmitter to represent function f , the modulator may generate up to L pre-processing functions φ_{kl} per transmitter. The physical layer frame (PHY frame) encompasses the generation of a passband signal $x_k^{pb}(t)$, which

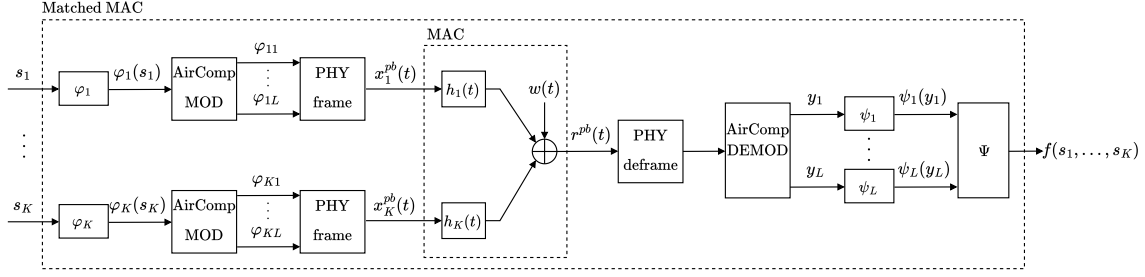


Fig. 1. Multiple access network of K distributed nodes implementing a modulation-based AirComp scheme.

is converted into a baseband signal at the receiver side by the corresponding deframing technique. The signal at the input of the receiver is

$$r^{pb}(t) = \sum_{k=1}^K h_k(t) \otimes x_k^{pb}(t) + w(t), \quad (7)$$

where \otimes corresponds to the convolutional operator, $h_k(t)$, $k = 1 \dots K$ are the passband channels, and $w(t)$ is the noise term at time t and has power σ_w^2 .

Under no noise, perfect channel conditions and perfect channel knowledge, the demodulation should undo the modulation functions such that the sum of the transmitted signals is obtained; this differs from a conventional communication system, where the demodulation must separately recover each of the transmitted signals. In this way, we can take advantage of the aggregation in the MAC in order to obtain an efficient system that does not require one orthogonal radio resource per transmitted signal. However, the receiver of an AirComp scheme faces more difficult conditions than a non-AirComp one. This motivates us to consider extra signal processing techniques. For this reason, AirComp demodulation does not necessarily correspond to standard analog or digital techniques. When discussing modulations for AirComp, we will also discuss what demodulation procedures are required.

First, in Sections III and IV, we assume perfect synchronization among all nodes, as well as perfect channel knowledge. Then, in Section VI, we assess the challenges that arise in AirComp techniques when these assumptions are not met.

C. Metrics

Given that the communication channel is not ideal, the receiver obtains \hat{f} , which is an estimate of the function f . Since the goal of AirComp is recovering a good estimate, the MSE is the first metric to consider:

$$MSE(\hat{f}) \triangleq E\{\|f - \hat{f}\|^2\}, \quad (8)$$

where the expectation is taken over the measurements and the channels. We also considers extensions of (8), such as the normalized MSE. Alternatively, a more informative metric is (9). Given a maximum tolerable error ε , the outage probability measures the probability of exceeding the interval of confidence that ε provides:

$$P_{out}(\hat{f}, \varepsilon) \triangleq \text{Prob} \left(|f - \hat{f}| \geq \varepsilon \right) . \quad (9)$$

When f is discrete, an error only happens when $f \neq \hat{f}$, i.e., the symbol is misclassified. We define the computation error rate as

$$P_{cer}(\hat{f}) \triangleq \text{Prob} \left(\hat{f} \neq f \right) . \quad (10)$$

Metrics (8) and (9) can be normalized, so that the difference between function values is normalized by the range of f .

Since the use of AirComp reduces the need of orthogonal signaling, latency is largely reduced. While in this work we provide the most relevant metrics used for AirComp, we refer the reader to [6] for a extensive review of all the different metrics used in AirComp.

It is important to note that depending on the application, there may be additional metrics that are not exclusively tied to AirComp. Therefore, each application needs to analyze how their specific metrics relate to the fundamental AirComp metrics outlined in this section. For example, in task-oriented communications, the age of information measures the timeliness of data. Another example is the accuracy and convergence rate of FEEL. However, these metrics not only vary depending on the application but are also currently under active research. Thus, we exclude them from the scope of this paper.

III. ANALOG MODULATIONS

While the current communication systems exclusively utilize digital modulations, there is interest in reintroducing analog modulations driven by joint source-channel coding schemes. Additionally, it is essential to acknowledge that many successful systems still rely on analog modulations, such as commercial frequency modulation (FM), or pulse position modulation (PPM) and pulse width modulation (PWM) for instrumentation systems. These considerations are pertinent as future communication systems will integrate computation and sensing, requiring a holistic view of modulation techniques beyond their current applications in broadband or 5G communication systems. Likewise, neural network systems empowered by the AI native framework may impose complexity and latency constraints, prompting a reevaluation of analog systems. Overall, it is crucial to keep these aspects in mind and to reopen discussions that may have seemed closed within the field of communications. Furthermore, the existing

literature is significantly confusing using the terminology for the modulated waveforms. In the following we clarify all these aspects.

A. Amplitude modulations

When multiple nodes transmit analog amplitude waveforms in a MAC, the resulting waveform corresponds to an aggregation of the baseband signals. This is due to the linear nature of these modulations. We first introduce analog schemes that modulate information that is continuous in amplitude and time. These may be implemented when the node gathers information continuously, such as in sensing applications. For double sideband (DSB) modulation, the information $\varphi_k(s_k)$ modulates the amplitude of the carrier as

$$x_k^{pb}(t) = A_k \varphi_k(s_k) \cos(2\pi f_c t), \quad (11)$$

where A_k controls the power of the transmitted signal by node k and f_c is the carrier frequency. The MAC aggregation in (7) particularized by (11) yields

$$r^{pb}(t) = \sum_{k=1}^K h_k(t) \otimes A_k \varphi_k(s_k) \cos(2\pi f_c t) + w(t). \quad (12)$$

Demodulation

In the case of an ideal channel, i.e., $h_k(t) = \delta(t)$ the amplitude of $r^{pb}(t)$ corresponds to the sum of the individual amplitudes. Thus, the multiple access scheme used to implement AirComp with amplitude modulations is direct aggregation (DA), this is, all users transmit simultaneously using the same radio source and the aggregation is performed seamlessly by the MAC. It also implies that the AirComp demodulation corresponds to the standard demodulation. For instance, in the case of DSB, this corresponds either to synchronous or envelope detection.

Since $L = 1$ is sufficient to compute f , the post-processing ψ is applied over the demodulated signal y and the aggregation function Ψ is redundant. Besides, the single sideband (SSB) modulation can be used to multiplex two signals simultaneously in the in-phase and quadrature components of the carrier.

As far as noise is concerned, DSB with ideal synchronous detection has the same performance as analog baseband AirComp, which is why linear modulations are implicitly considered in all works that solely develop AirComp techniques in baseband [16], [19]–[21]. However, the performance depends on the computed function because the post-processing may alter the noise characteristics. For instance, the exponential post-processing required to compute the geometric mean (see Table I), whenever it is possible to apply a logarithmic pre-processing, transforms the additive Gaussian noise into multiplicative and log-normal, which highly degrades the signal.

The high demand on power efficiency incorporated analog pulse modulations. By incorporating a time sampler, the waveforms are generated by modulating the samples into pulses. Pulse-based modulations are also useful to optimally multiplex data in time. For instance, in FEEL, each transmitter needs to send large amounts of parameters, which can be transmitted as a train of pulses. Alternatively, pulses are relevant in surveillance and IoT applications, characterized by event-sampling [22].

Without loss of generality, we assume the transmission of a pulse every T . In analog pulse amplitude modulation (PAM), the transmitted waveform corresponding to a single pulse is

$$x_k^{pb}(t) = A_k \varphi_k(s_k) p(t), \quad (13)$$

where $p(t)$ is a finite-energy pulse of duration T . Since PAM implements DA as a multiple access scheme, the AirComp demodulation follows the standard PAM demodulation (e.g., low-pass filtering).

While amplitude modulations seem the perfect choice for AirComp, from the signal processing perspective, they may not be ideal from the communication point of view. In practice, the transmitted power depends on the data and requires tight channel state information (CSI) to ensure the superposition required by AirComp. Overall, these aspects may push the power amplifier outside the linear region and incur high energy consumption.

B. Angular modulations

Angular modulations place the information in the argument of the carrier. In the case of continuous-time information signals, these correspond to the classical frequency modulation FM or phase modulation (PM). Alternatively, the analog information can modulate the position or the width of transmitted pulses, thus, receiving the name of PPM or PWM, respectively. The interest in angular modulations stems from the fact that these exhibit better performance than amplitude modulations. For instance, FM requires moderately complex circuitry, while the signal-to-noise ratio (SNR) can be increased arbitrarily consuming more bandwidth (i.e., the so-called power-bandwidth exchange) [23]. However, due to their non-linear nature, the sum provided by the radio channel over the waveforms does not result in the sum of the corresponding arguments, i.e., $e^{ja} + e^{jb} \neq e^{j(a+b)}$. Nonetheless, although to date, there is no multiple access scheme that integrates analog angular modulations for AirComp, in the next section it will be shown that this does not prevent the applicability of digital angular modulations.

IV. DIGITAL MODULATIONS

Consider the digital transmission architecture in Fig. 2. First, in the source encoder, the input information goes through an analog-to-digital converter (ADC) that discretizes both in time and amplitude.

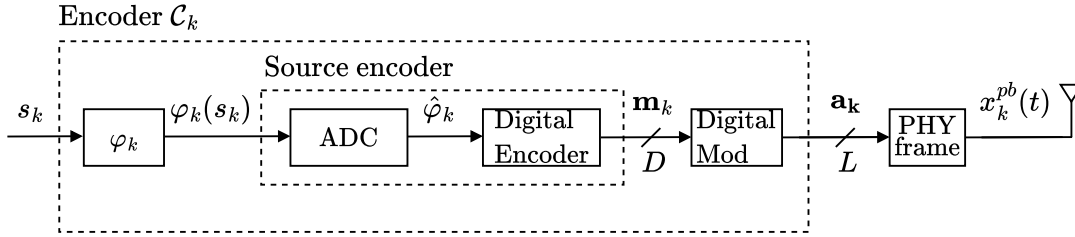


Fig. 2. AirComp transmitter implemented with digital modulations.

We assume an M -level uniform quantizer, and $\hat{\varphi}_k \in [0, M - 1] \subset \mathbb{N}$ to be the quantized symbol. The next block of the source encoder is a digital encoder, that outputs a digital representation of the data $\mathbf{m}_k \in \mathbb{R}^D$. Historically, this has followed a binary representation, although we will show that, for the purpose of AirComp, alternative numeral systems may be useful. Thus, for each quantized level, we consider that a vector of $D \leq L$ digits is generated. Note that this implies that from a single $\hat{\varphi}_k$, the source encoder has generated D components, which can be identified with each of the pre-processing functions φ_{kl} .

The vector \mathbf{m}_k is fed to a digital modulator that maps it to symbols $\mathbf{a}_k \in \mathbb{C}^L$ of a constellation. In traditional communication systems, this design depends on the rate that can be accommodated by the physical channel and on the desired BER. Alternatively, for AirComp, the constellation design has to be performed according to the AirComp goals (e.g., MSE). Finally, each of the resulting symbols \mathbf{a}_k are fed to the physical layer frame, which does not only take care of pulse shaping, power control, and up-conversion for passband transmission, but also of building advanced modulation formats either for multiplexing or for diversity, such as multicarrier, spread spectrum modulations or multi-antenna processing. Pilot sequences or any other redundancy (e.g., cyclic prefix) are also introduced following the standard's physical layer protocol frame.

Note that in a practical wireless transmitter \mathbf{m}_k goes through a channel encoder, which introduces techniques to make the transmitted information robust to channel impairments. Fig. 2 omits it because this paper does not deal with its specific design in order to keep the scope.

In the following, we will introduce the existing digital modulations that can be implemented for AirComp, along with the corresponding multiple access frameworks.

A. Amplitude modulations

As with analog amplitude modulations, digital amplitude modulations also match the additive nature of the MAC. Consider a digital unipolar PAM with a normalized symbol amplitude of 1, such that

$a_k \in [0, 1, \dots, M - 1]$. For this scheme to work in an AirComp setup, there must be a linear mapping between the quantized levels $\hat{\varphi}_k$ and the PAM symbols a_k , to preserve the additive nature of the MAC. Notice that breaking the linearity of the encoding (e.g., Gray code) results in a non-linear map from $\hat{\varphi}_k$ to a_k , which will produce overlaps of different aggregations. In the case that the input variable has both positive and negative values, the modulation to be used is the digital polar PAM. When the symbols are transmitted with a radio frequency pulse, it yields the amplitude-shift keying (ASK) modulation.

Demodulation

Notice that the receiver cannot use the same codebook for demodulation, since new symbols emerge due to the superposition of symbols. For instance, with $K = 2$ transmitters, $a_1 = 1$ and $a_2 = M - 1$, the received symbols is M , which does not exist at the encoder side. As with analog modulations, two M -ary ASK signals can be multiplexed in the phase and quadrature components of the waveform, which results in M^2 -ary quadrature amplitude modulations (QAM). The main drawback of these schemes is that the codebook at the receiver depends on the number of users K .

Alternatively, the sum can be performed at the digit level as in [10], [15]. For example, consider the quantized readout $\hat{\varphi}_k$ expressed in a p -ary system: $\hat{\varphi}_k = \sum_{d=0}^{D-1} p^d m_k^{(d)}$, where $m_k^{(d)} \in \mathbb{Z}_p$ is the d -th digit of $\mathbf{m}_k \in \mathbb{Z}_p^D$. When particularized for the binary case, $p = 2$, $m_k^{(d)} \in \{0, 1\}$ and the digital modulator maps each bit to a binary polar PAM symbol, i.e., $a_k^{(d)} = 1 - 2m_k^{(d)}$. Notice that the transmission of D digits requires the transmission of D symbols multiplexed in D orthogonal radio resources. Therefore, in this case, where AirComp implements an aggregation over digits, the original measurement s_k has been decomposed into D pre-processed values $\varphi_{kl} = a_k^{(l)}$, with $D = L$, which will be transmitted over the MAC orthogonally.

The corresponding received signal at resource l after transmission through an ideal channel and demodulation is

$$y_l = \sum_{k=1}^K a_k^{(l)}. \quad (14)$$

The sum of the l -th bit is equivalent to $\sum_{k=1}^K m_k^{(l)} = (K - y_l)/2$. Finally, as shown in (15), the arithmetic mean can be recovered by transforming the averaged L bits to a decimal base. According to Fig. 1, equation (15) encompasses both the post-processing ψ_l as well as the aggregation Ψ . The former corresponds to $\psi_l = 2^l(K - y_l)/2K$, whereas Ψ is a sum.

$$\frac{1}{K} \sum_{k=1}^K \hat{\varphi}_k = \frac{1}{K} \sum_{k=1}^K \sum_{l=1}^L 2^l m_k^{(l)} = \frac{1}{K} \sum_{l=1}^L 2^l \sum_{k=1}^K m_k^{(l)} = \frac{1}{K} \sum_{l=1}^L 2^l \frac{K - y_l}{2} \quad (15)$$

In [24], it is shown that the operation can lead to a carry, which requires the adoption of broader non-binary representations ($p > 2$). These aspects are revised in Subsection IV-C, which introduces modulations with more degrees of freedom.

B. Angular modulations

As in analog angular modulations, a digital angular modulation does not provide an aggregated signal that is linear with respect to the modulated information. However, modulations that offer an orthogonal waveform support, e.g., frequency-shift keying (FSK) and PPM, can be integrated into AirComp with the use of a multiple access scheme termed type-based multiple access (TBMA) [25]. This scheme exploits the fact that symmetric functions can be computed from the type (i.e., histogram) of the data. The intuition behind TBMA is a one-to-one mapping between L different measurements and L orthogonal radio resources. Thus, in TBMA, radio resources are assigned according to data, which allows superposition when users have the same measurement, as it is explained next in the demodulation process.

Demodulation

After simultaneous transmission, the demodulation procedure corresponds to a bank of matched filters at the L waveforms. The aggregated signal after demodulation (i.e., y_1, \dots, y_L in Fig. 1) represents a histogram of the used radio resources, which equivalently corresponds to a histogram of the transmitted data. To compute f , the authors of TBMA propose an estimator for the received data distribution that asymptotically approaches the maximum likelihood estimator. Thus, it is consistent and efficient [25]. Notice that, unlike traditional digital schemes, the TBMA demodulation corresponds to a bank of matched filters, whose outputs are used to estimate f .

In Fig. 3 we present how to build a FSK-based TBMA system for AirComp. To build a one-to-one mapping between the measurement and the radio resource spaces, the number of levels in the quantizer is set to $M = L$ and each \mathbf{m}_k is mapped to a unique symbol \mathbf{a}_k . Under this framework, superposition over the MAC happens for all nodes transmitting the same quantized readout m_k . Since TBMA requires orthogonal signaling, it can be implemented with M orthogonal frequencies, f_k over M -ary FSK [26].

The receiver deploys a bank of filters at the L frequency bands, which can be implemented with a discrete Fourier transform (DFT) of L samples. The received signal after demodulation, y_l corresponds to a noisy version of the number of nodes with the same measurement. In this case, TBMA incurs in single-shot transmission by all users at the expense of an increased occupied bandwidth. Instead of using

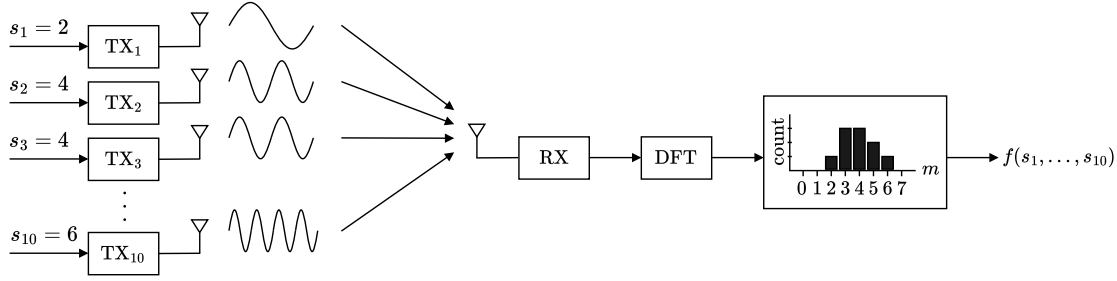


Fig. 3. Example of a TBMA implementation with FSK in an ideal channel. We consider $K = 10$ nodes with the following data: (2, 3, 3, 3, 4, 4, 4, 5, 5, 6). The system is designed with $M = 8$ and each node transmits an FSK carrier according to each measurement. At the receiver side, a bank of matched filters is implemented with the DFT, and the result is a histogram of each waveform or measurement. The function is computed from the type.

the TBMA estimator, one can alternatively compute the function from the received data. For instance, the arithmetic mean can be computed as

$$\Psi(\psi_l(y_1), \dots, \psi_l(y_L)) = \frac{1}{K} \sum_{l=1}^L ly_l, \quad (16)$$

where $\psi_l = ly_l/K$ and Ψ corresponds to the sum. Notice that the aggregation does not necessarily correspond to the mean or even a linear function. For instance, the geometric mean can be computed as

$$\Psi(\psi_l(y_1), \dots, \psi_l(y_L)) = \exp \left(\sum_{l=1}^L \frac{y_l}{K} \ln(l) \right), \quad (17)$$

Furthermore, TBMA can be implemented at the bit level by assigning two orthogonal symbols (i.e., two radio resources) to each bit. The receiver recovers the type over each bit, which is used to compute the sum. For signed variables, two's complement representation of integers can be used. This idea was exploited in [24] with a generic numeral system, and in [27] with a balanced number system to take the negative-valued parameters into account.

TBMA provides more information at the receiver side at an expenses of a higher radio resource consumption. Having access to the type and not just to a single aggregation by DA allows to compute multiple functions in a single transmission, as seen with (16) and (17).

While linear analog modulations are an estimation problem, TBMA depends on the function of interest. For instance, the arithmetic mean in (16) corresponds to an estimation problem, while the maximum function corresponds to a detection. This is because the latter boils down to detecting the signal associated with the largest radio resource. This also implies that, depending on the function and how it is implemented, the metric needs to be chosen carefully as well. In estimation problems, one is interested in the MSE in (8), while in detection, the error rate in (10). Note, however, that TBMA is

not the only possibility for AirComp access when using angular modulations. Use Case 1 discussed next illustrates this with an example.

Use case 1: New angular modulations for DA

Consider that, instead of adding waveforms, these are multiplied:

$$\cos(2\pi f_1 t) \cdot \cos(2\pi f_2 t) = \cos(2\pi(f_1 + f_2)t) + \cos(2\pi(f_1 - f_2)t) \quad (18)$$

There is a term in which the individual frequencies are added, which is the desired output of AirComp. To achieve this product, we can transform the additive channel into a multiplicative one. As seen in Table I, a sum turns into a product with a logarithmic preprocessing and an exponential postprocessing. If we apply the preprocessing step over the waveform, the result is

$$x_k(t) = A_k \log \left(\sqrt{\frac{2}{T}} \cos \left(\frac{\pi(2m_k + 1)}{2T} t \right) + \alpha \right), \quad (19)$$

and the exponential postprocessing is computed at the receiver side. This waveform, termed logarithmic FSK (Log-FSK), uses the Kolmogorov-Arnold superposition theorem to design the waveform and the function [28] simultaneously. With this, the matched MAC allows to implement DA with angular modulations. In light of (18), the demodulation procedure still requires a bank of filters and detecting the maximum frequency component, this is, where the AirComp result happens. Since the amplitude is not relevant, Log-FSK performs a pure digital demodulation.

Use case 2: A hybrid analog and digital modulation for function approximation

Consider a single transmitter with data m , that needs to compute a function $f(m)$. While the discrete cosine transform (DCT) has been widely used to approximate and compress signals (see Fig. 4), its sinusoidal nature can be also exploited as a waveform. In [29], an additional time index is appended to the inverse DCT expression to transform it into a hybrid amplitude and angular modulation. The baseband transmitted signal is

$$x(t) = A_c \sqrt{\frac{2}{N}} \sum_{q=1}^Q F_q \cos \left(\frac{\pi q(2m + 1)}{2T} t \right), \quad (20)$$

where F_q , $q = 1, \dots, Q$ are the DCT coefficients that characterize function $f(m)$. The modulation is hybrid because it carries information in both the amplitude and the frequency of the signal. Thus, the waveform inherits the benefits from the DCT representation. Fig. 5 shows the MSE to compute the sigmoid function with $Q = 3$. The DSB carries $f(s)$ in the amplitude of the carrier, while FSK corresponds to (20) without the amplitudes, which are imposed at the receiver side.

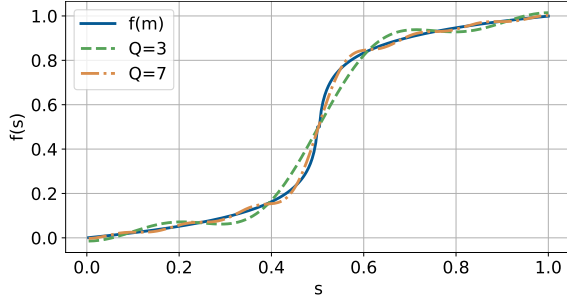


Fig. 4. Sigmoid function and its DCT approximation with $Q = 3$ and 7 coefficients.

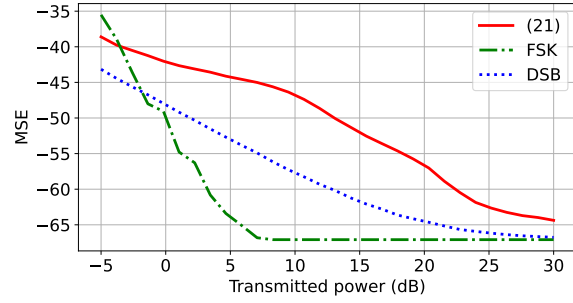


Fig. 5. MSE in an AWGN channel to approximate $f(s)$ with $Q = 3$.

C. Hybrid amplitude and angular modulations

In Use Case 2 from Section IV-B we have introduced a hybrid modulation to approximate a function in a communication channel. Hybrid modulations allow one to design both the amplitude and the angle of the waveform. While standard amplitude phase-shift keying (APSK) modulations, such as QAM, are not suitable for AirComp due to destructive overlaps among the superimposed constellation points, these can be overcome by appropriately designing the digital modulator (see Use Case 3).

Following a more general approach, the goal is to uncover a proper choice for designing the digital modulator and pre-processing jointly so that DA can be implemented for hybrid modulations. This joint design is performed by a set of encoders \mathcal{C}_k and the decoder \mathcal{D} (see Fig. 2). If the optimum criterion is the minimum MSE, it reads as:

$$\mathcal{C}_1^*, \dots, \mathcal{C}_K^*, \mathcal{D}^* = \underset{\mathcal{C}_1, \dots, \mathcal{C}_K, \mathcal{D}}{\operatorname{argmin}} \sum_{n=1}^N \left\| f(s_1, \dots, s_K) - \Psi(\psi_1(y_1[n]), \dots, \psi_L(y_L[n])) \right\|_2^2. \quad (21)$$

where \mathcal{D} denotes the AirComp demodulation in Fig. 1.

Since we are using digital modulations, let R_f denote the number of all possible discrete values in the range of function f and $s_k^{(i)}$ taking on one of R_f possible values. Moreover, we define $f^{(i)}$ to be i -th output of the function f for a given set of quantized input values $s_1^{(i)}, s_2^{(i)}, \dots, s_K^{(i)}$. Next, we use $r^{(i)}$ to present the constellation points corresponding to i -th output value, i.e., $r^{(i)} = \sum_{k=1}^K a_k^{(i)}$, where $a_k^{(i)} \in \mathbb{C} \forall (i, k)$. Then, it is crucial that if $f^{(i)}$ differs from $f^{(j)}$ (j -th output value), their respective constellation points $r^{(i)}$ and $r^{(j)}$ must also be different. These conditions can be rewritten into the following feasibility optimization problem:

$$\text{find } a_1^{(i)}, \dots, a_K^{(i)} \text{ s.t. if } f^{(i)} \neq f^{(j)} \Rightarrow r^{(i)} \neq r^{(j)}, \forall (i, j), |a_k^{(i)}|^2 \leq P_k, \forall (i, k) \quad (22)$$

Generally, (22) is difficult to solve because it is highly non-convex and non-smooth. The authors

in [30] approach it in an intuitive fashion. Specifically, they investigate the bit-wise majority function $f = \text{sign}(\sum_{k=1}^K \text{sign}(s_k))$, by controlling the phase values in binary phase-shift keying (BPSK). More specifically, for binary input values, $m_k^{(i)} = \{0, 1\}$, the modulator becomes:

$$a_k^{(i)} = A_k^{(i)} \left(1 - 2m_k^{(i)}\right), \quad \forall(i, k), \quad (23)$$

where the scalar $A_k^{(i)} \in \mathbb{C}$ has unit power. The imposition of the sign function constraint leads to a reduced number of feasible constellation diagrams, since f is only either 0 or 1. Consequently, instead of solving the optimization in (22), we can determine the transmitter phase shifts $A_k^{(i)}$ satisfying the constraints in (22) through an exhaustive search that yields the lowest BER.

On the other hand, the authors in [31] study the general optimization in (22) for AirComp. The non-convex and non-smooth constraints in (22) can be replaced with a smooth condition,

$$\begin{aligned} a_1^{(i)}, \dots, a_K^{(i)} &= \underset{\epsilon, a_1, \dots, a_K}{\text{argmax}} \epsilon, \\ \text{s.t.} \quad &\left| \sum_{k=1}^K a_k(m_k^{(i)}) - \sum_{k=1}^K a_k(m_k^{(j)}) \right|^2 \geq \epsilon |f^{(i)} - f^{(j)}|^2, \forall (i, j) \end{aligned} \quad (24a)$$

$$|a_k(m_k^{(i)})|^2 \leq P_k, \quad \forall(i, k) \quad (24b)$$

where P_k is the power budget for the constellation diagram at node k . Note that for any sufficiently small ϵ , the solution to (24) equals the solution to (22). The optimization problem in (24) is a quadratic programming problem with non-convex constraints, known to be NP-hard [32]. Fortunately, this is a well-studied optimization that several approximation techniques have been developed to overcome the non-convex constraint, such as semi-definite relaxation [33] and Gaussian randomization methods [34]. Fig. 6 shows an example of the resulting constellations.

Demodulation

After solving the optimization problem in (24), the receiver needs to design the decision boundaries using the maximum likelihood estimator. Since the resulting constellation depends on the function, the corresponding de-mapper $\mathcal{D}(\cdot)$ changes with f and K .

The main drawback of this approach is the complexity of solving such a non-convex optimization problem in (22). To mitigate the design complexity, one effective approach is to confine the desired function to be the sum function, and limit the modulation optimization solely on the sum function [35]. This allows the use of the same mapper $\mathcal{C}_k(\cdot) = \mathcal{C}(\cdot)$ across all nodes. Although not mandatory, the modulation mapper's capability to function as an additive map can simplify further the procedure.

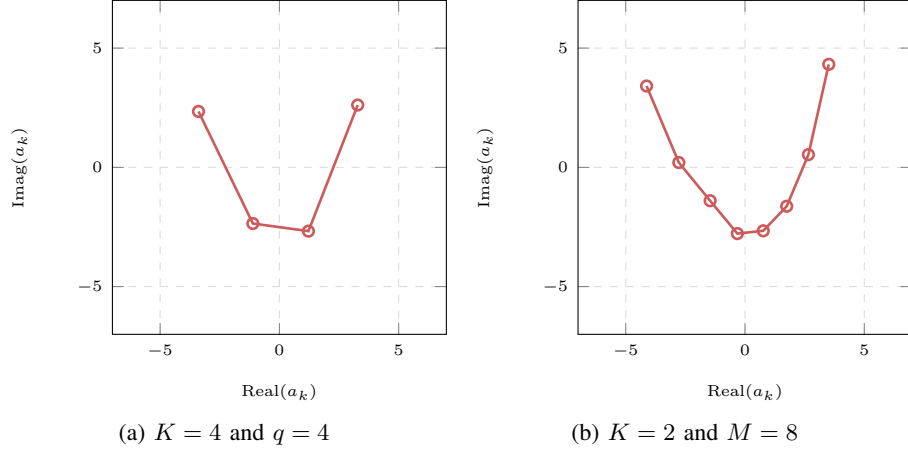


Fig. 6. Constellation diagram of the modulation vector for the product function $f = \prod_{k=1}^K x_k$ in different setups.

In this context, the linearity of the nested lattice codes makes them suitable for accurately mapping inputs to constellation points. It is important to note that employing lattice codes for the transmitted symbols results in the superposed symbol at the receiver deviating from the input lattice field. Therefore, distinct from standard employed lattice codes in digital AirComp [17], the focus shifts to the received codewords rather than the combination of transmitted codewords. This adjustment can potentially simplify the decoding process as [24] shows, enabling also the straight forward adoption of low-density parity check channel coding (LDPC) schemes.

Use case 3: DA with angular modulations

It is challenging to implement DA with existing digital modulations, as the aggregation of symbols generates overlaps that correspond to different function values. However, these modulations can implement DA for specific cases, such as the BPSK, which corresponds to a binary polar PAM, as in (14). The extension to higher-order modulations is cumbersome but not impossible. Fig. 7 shows the use of quadrature phase-shift keying (QPSK) modulations for $K = 2$ and $\hat{\varphi}_k = \{-2, -1, 1, 2\}$. In the left figure, an appropriate mapping of $\hat{\varphi}_k$ to the constellation symbols a_k make it possible to use AirComp. While overlaps occur, these correspond to the same function value, which does not generate any ambiguity at the receiver side. Conversely, in the right figure, we show that not every modulation mapping is possible. Switching two symbols results in a destructive overlap that the receiver cannot resolve, as well as two redundant symbols (i.e., 3). Furthermore, extending this encoding for $K > 2$ is not guaranteed to work. In general, the number of overlaps and redundancies will increase with K .

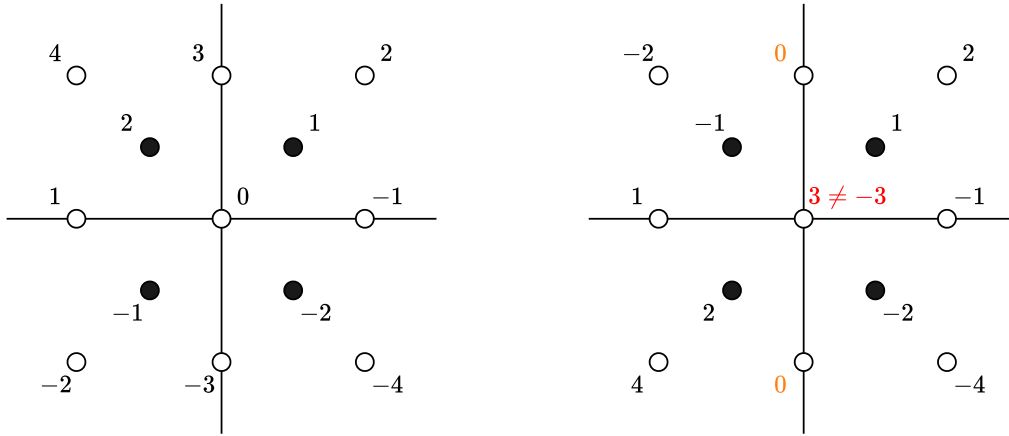


Fig. 7. Constellation diagram showcasing the transmission and reception of QPSK signals by two nodes ($K = 2$) to compute the sum. The black dots correspond to the constellation used for transmission, while the white dots correspond to the constellation at the receiver side, i.e., after AirComp superposition. We assume $\varphi_k = \{-2, 1, 1, 2\}$ and propose two different modulation mappings to symbols.

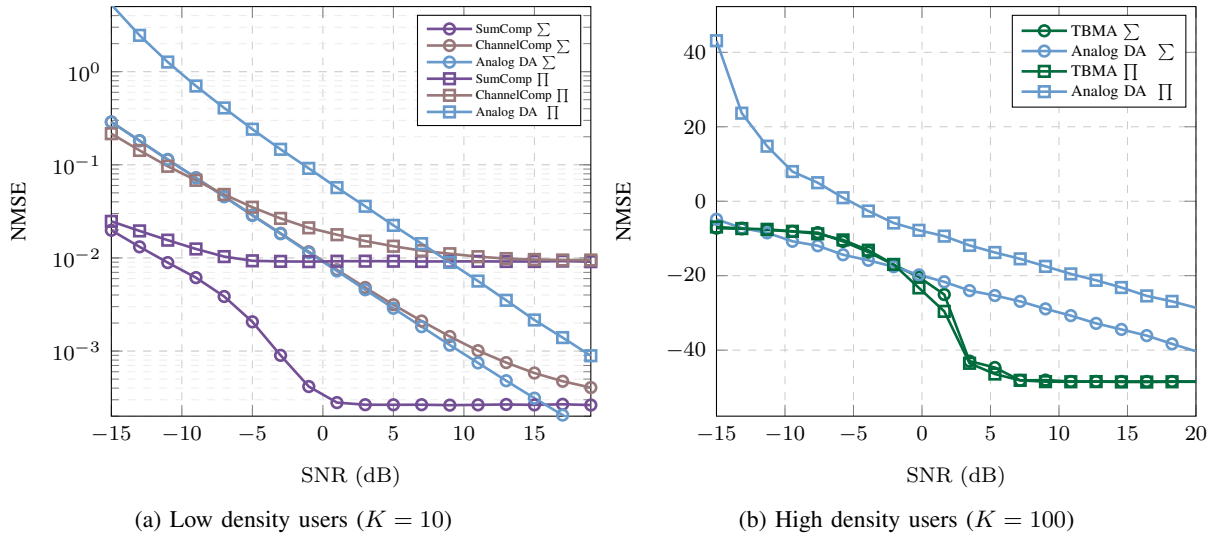


Fig. 8. Performance comparison of different AirComp schemes for the arithmetic ($Q = 64$) and geometric mean ($Q = 8$) functions. In Fig. 8a we compare DA schemes in the analog and digital domain. In Fig. 8b we compare TBMA ($Q = 64$) to analog DA. The input values are generated $s_k \sim \mathcal{U}[1, 64]$ for the mean function and $s_k \sim \mathcal{U}[1, 8]$ for the geometry mean function. The normalized MSE is averaged over 5×10^4 Monte Carlo trials.

D. Summary

Table II summarizes which are the modulations that have been so far used in the literature of AirComp. We highlight that analog angular modulations are not suitable for AirComp, while existing digital angular modulations can be used with TBMA. Furthermore, the development of new modulations for AirComp is a promising field of research. Use case 4 illustrates the integration of modulations for the application

TABLE II
SUMMARY OF MODULATIONS FOR AIRCOMP.

Modulation	Category	Multiple Access	References
SSB	Amplitude	DA	None
Analog PAM	Amplitude	DA	[16], [19]–[21]
Digital PAM	Amplitude	DA	[10]
FSK	Angular	TBMA	[24], [26], [27]
Digital PPM	Angular	TBMA	[36]
Log-FSK	Angular	DA	[28]
Hybrid amplitude-angular	Amplitude-angular	DA	[15], [31]

of FEEL.

Fig. 8 compares the performance of the presented modulations for two different functions, namely, the arithmetic and geometric means. Since the presented hybrid modulations change the constellation depending on the number of nodes K , and the optimization problem becomes harder to solve for an increasing K , it is best suit for scenarios with a low density of users. Conversely, the configuration of TBMA is independent of K and highly benefits from similar measurements, which suits scenarios with high density of users.

Use case 4: Modulations for FEEL

FEEL is the leading application for AirComp in the literature. See Section II-A for a brief description of the working procedure of FEEL. To average the model parameters, i.e., f is the arithmetic mean, one choice is to use amplitude modulations [19]. Alternatively, M -ary FSK can be used to implement TBMA [37]. Furthermore, FEEL can be realized by averaging the gradients rather than the model parameters. In [38], each gradient is quantized with a single bit (i.e., sign of the gradient) and encoded into a BPSK waveform. At the receiver side, the sign of the waveform is recovered, rather than the magnitude. In this case, f corresponds to the majority voting, which is more robust to noise and hardware friendly. However, as in the previous approaches, this still corresponds to an amplitude aggregation and requires CSI to compensate the channel. To overcome these issues, in [36], the sign of the gradient is encoded with binary FSK and implemented with TBMA. Computing the majority voting over binary TBMA is achieved with an energy detector that compares both received signals (see Fig. 9). This allows to implement a CSI-free AirComp scheme for FEEL.

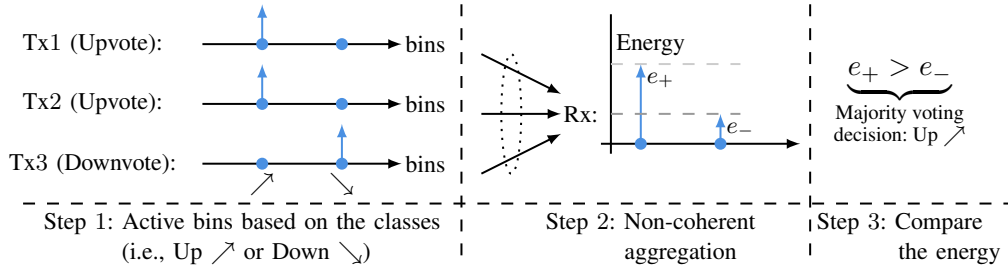


Fig. 9. An example of computing a quantized majority voting function with non-coherent AirComp. Bins can be subcarrier indices (i.e., FSK), chirp indices (i.e., CSK), or indices in time (i.e., PPM).

V. PHYSICAL LAYER FRAME

In its basic conception, the physical layer (PHY) frame handles pulse shaping, carrier modulation and transmitted power control, so that in each transmitter $k = 1 \dots K$ from the digital symbols a_k the transmitted waveform $x_k^{pb}(t)$ is produced as¹:

$$x_k^{pb}(t) = \Re \left\{ \sum_{n=1}^{\infty} A_c a_k[n] p(t - nT) e^{j2\pi f_{tx,k} t} \right\}, \quad (25)$$

where A_c is the amplitude transmitted by the power control, $\frac{1}{T}$ determines the transmission bandwidth, $p(t)$ is the pulse shape of finite energy $E_p = 1$ J, and the carrier frequency $f_{tx,k}$ is a integer multiple of $\frac{1}{T}$. However, the PHY frame also constructs sophisticated modulation schemes for multiplexing or diversity. That is, the PHY frame adapts the baseband symbols a_k for passband transmission and makes them robust against impairments (e.g., interferences, multipath, noise,...). To achieve these, the PHY frame uses extra radio resources to provide a processing gain at the receiver side. For instance, when Q readouts in one terminal are to be multiplexed, a serial to parallel conversion takes place in the PHY frame so that each one maps to a different carrier (i.e., Orthogonal Frequency Division Multiplex - OFDM) or, antenna (i.e., Multiple Input Multiple Output - MIMO) or code (i.e., Code Division Multiple Access - CDMA). Although under ideal transmission conditions, the PHY frame and de-frame (i.e., at the receiver) processes must be transparent to the function computation, these schemes are revisited in next section due to their importance in AirComp when dealing with the channel impairments. Note that in AirComp the time synchronization and CSI requirements at each of the transmitters are more critical than in a conventional MAC scheme, which does not aim to compute any function. We demonstrate the indispensability of OFDM schemes in easing these demands. As an alternative, a variation of CDMA,

¹We are not considering in this model the case of event-based transmission, where T is then a random variable. M -ary continuous phase FSK signals with $M > 2$ are not encompassed by this model either.

as outlined in [20], is suggested to render the resultant scheme resilient against synchronization errors at both time and phase levels. In this approach, each readout s_k , whether analog or digital, modulates a random sequence of length Q . Besides, multi-antenna or MIMO signal processing and optimization must be differently approached in AirComp as next section will also point out. Note that multiplexing schemes are particularly useful in applications with large amounts of data (e.g., FEEL) in order to reduce latency, and that whenever the frequency domain is used, the demodulator must implement TBMA.

Spread spectrum techniques are very useful in combating interference. In [37] the symbol a_k is modulated in the frequency of a chirp spread spectrum (CSS) signal, which corresponds to the long range (LoRa) modulation. Overall, the range of signal processing techniques to be devised in the PHY frame for AirComp is huge and constitutes quite a virgin research field.

VI. CHALLENGES OF MULTIPLE ACCESS CHANNELS FOR AIRCOMP

In wireless communication networks, practical systems encounter challenges that significantly diverge from ideal models represented in (2). These include hardware impairments, propagation distortions such as path loss, shadowing, multipath fading, thermal noise, and network interference. Such issues are aggravated by synchronization errors among the wireless units. Additionally, incorporating physical parameters and practical limitations into modeling processes is crucial to represent realistic wireless channels accurately. In what follows, we give a general system model for the fading MAC with a detailed exploration of each term provided in subsequent subsections.

In particular, let $x_k(t) \in \mathbb{C}$ be the baseband signal for the k -th transmitter. Hence, the passband signal of the k -th transmitter that is formulated in (25) can also be expressed as

$$x_k^{pb}(t) = \Re\{x_k(t)e^{j2\pi f_{ix,k}t}\} \quad k \in [K]. \quad (26)$$

Assume that the impulse response of the multi-path channel in the passband is given by

$$h_k(t) = \sum_{p=1}^P h_{k,p}^c \delta(t - \tau_{k,p}), \quad (27)$$

where P is the number of paths, $h_{k,p}^c \in \mathbb{R}$ and $\tau_{k,p} \in \mathbb{R}$ are the p -th path gain and path delay for the k -th transmitter, respectively. The received passband signal $r^{pb}(t)$ can then be expressed as

$$r^{pb}(t) = \sum_{k=1}^K h_k(t) \otimes x_k^{pb}(t) + w(t) \quad (28)$$

The following subsections will explore the signal processing techniques that take place at the physical layer framing and at reception under different scenarios of fading effects and CSI availability.

A. Full CSI availability

We recall that the symbol a_k at sensor k modulates $\varphi_k(s_k)$ by using encoder $\mathcal{C}_k(\cdot)$, i.e., $a_k = \mathcal{C}_k(\varphi_k(s_k))$ for transmitting over the MAC. The symbols are then properly framed into a physical layer waveform. Afterward, the received signal $r^{pb}(t)$ is translated to baseband, $r(t)$, sampled at symbol rate T to produce $r[n]$, and further processed by the system \mathcal{D} , resulting in the output signals y_l , i.e.,

$$y_l = \mathcal{D}\{r[n]\}, \quad l = 1, \dots, L. \quad (29)$$

Throughout this section we assume $L = 1$ and f corresponds to the sum or arithmetic mean. Moreover, the following techniques only apply to linear analog modulations, for which DA is also assumed. To simplify exposition, the channels are assumed to have slow fading such that their states remain constant without the communication window. The extension to time-varying channels can be found in [21].

1) *Power control*: In light of the previous assumptions, we can rewrite (1) as

$$y = \sum_{k=1}^K h_k b_k s_k + w, \quad (30)$$

where b_k is the precoder that takes care of the power control. Note that (30) assumes a linear model for the preprocessing function, namely, $\varphi_k(s_k) = b_k s_k$. Channel-inversion power control is typically applied to achieve the magnitude alignment required for AirComp [19], [38]. However, *is channel inversion the optimal strategy for AirComp?* Considering an arbitrary symbol slot, this strategy is to set the transmitted symbols as

$$b_k = \begin{cases} \rho_0 h_k^* / |h_k|^2, & |h_k|^2 \geq g_{\text{th}}, \\ 0, & |h_k|^2 < g_{\text{th}}, \end{cases}, \quad (31)$$

where ρ_0 scaling factor is set to satisfy the average transmit power and g_{th} is a channel-truncation threshold to cope with deep fading. A quick answer to the initial question is negative in practice where sensors are typically power constrained. To be more elaborate, the optimal strategy exhibits a *threshold-based* structure such that a transmitter applies channel-inversion power control if its *quality indicator*, which accounts for both its power budget and channel power gain, exceed the threshold; otherwise, full power transmission should be performed [21]. The detailed mathematical analysis and the resultant detailed optimal strategy are presented in the sequel.

If we set $\rho_0 = p_k$, where $p_k \geq 0$ denotes the transmit power at device k , and perform channel inversion

for all users, (30) turns into

$$y = \sum_{k=1}^K \sqrt{p_k} |h_k| s_k + w. \quad (32)$$

Upon receiving the signal y , the receiver applies the denoising factor η , to recover the average message of interest as $\hat{f} = y/K\sqrt{\eta}$. Then, the AirComp error is given as

$$\text{MSE}(f) = \frac{1}{K^2} \mathbb{E} \left[\left(\frac{y}{\sqrt{\eta}} - \sum_{k=1}^K s_k \right)^2 \right] \quad (33)$$

Our objective is to minimize (33) by jointly optimizing the power control p_k at devices and the denoising factor η subject to the individual average transmit power constraints. This result in the following power control problem:

$$\begin{aligned} (\mathbf{P1}) : \quad & \min_{\{p_k \geq 0\}, \eta \geq 0} \sum_{k \in \mathcal{K}} \left(\frac{\sqrt{p_k} |h_k|}{\sqrt{\eta}} - 1 \right)^2 + \frac{\sigma^2}{\eta} \\ & \text{s.t.} \quad p_k \leq \bar{P}_k, \quad \forall k. \end{aligned}$$

It is observed that the objective function of problem (P1) consists of two components: the signal misalignment error, and the noise-induced error, respectively. In general, adjusting η induces a *fundamental tradeoff* between minimizing the signal misalignment error and suppressing the noise-induced error. It is evident that the optimal power-control policy to problem (P1) for device k is given by

$$p_k^* = \min \left(\bar{P}_k, \frac{\eta}{|h_k|^2} \right). \quad (34)$$

Next, we proceed to optimize over η . By substituting p_k^* in (34) into problem (P1), we have the optimization problem over η as

$$\min_{\eta \geq 0} \sum_{k=1}^K \left(\min \left(\frac{\sqrt{\bar{P}_k} |h_k|}{\sqrt{\eta}} - 1, 0 \right) \right)^2 + \frac{\sigma^2}{\eta}, \quad (35)$$

Even though a closed-form solution is difficult, its structure can be characterized by studying the properties of the objective function, e.g., its unimodality [21]. To solve problem (35), we need to remove the minimum operation to simplify the derivation. To this end, we find it convenient to adopt a *divide-and-conquer* approach that divides the feasible set of problem (35), namely $\{\eta \geq 0\}$, into $K + 1$ intervals. Note that each of them is defined as

$$\mathcal{F}_k = \{ \eta \mid \bar{P}_k |h_k|^2 \leq \eta \leq \bar{P}_{k+1} |h_{k+1}|^2 \}, \quad \forall k \in \{0\} \cup \mathcal{K}, \quad (36)$$

where we define $\mathcal{K} = \{1, \dots, K\}$, $\bar{P}_0|h_0|^2 \triangleq 0$ and $\bar{P}_{K+1}|h_{K+1}|^2 \rightarrow \infty$ for notational convenience. Then, it is easy to establish the equivalence between the following two sets:

$$\{\eta \geq 0\} = \bigcup_{k \in \{0\} \cup \mathcal{K}} \mathcal{F}_k. \quad (37)$$

Given (37), we note that solving problem (35) is equivalent to solving the following $K + 1$ subproblems and comparing their optimal values to obtain the minimum one:

$$\min_{\eta \in \mathcal{F}_k} F_k(\eta) \triangleq \sum_{i=1}^k \left(\frac{\sqrt{\bar{P}_i}|h_i|}{\sqrt{\eta}} - 1 \right)^2 + \frac{\sigma^2}{\eta}, \quad \forall k \in \{0\} \cup \mathcal{K}, \quad (38)$$

with $F_k(\eta)$ denoting the objective function of the k -th subproblem. Notice that when $k = 0$, we have $F_0(\eta) = \sigma^2/\eta$. In addition, we have

$$F(\eta) = F_k(\eta), \quad \forall \eta \in \mathcal{F}_k, \quad \forall k \in \{0\} \cup \mathcal{K}. \quad (39)$$

With the optimal index k^* that can be found by the search, the optimal power control over static channels that solves problem (38) has a threshold-based structure, given by

$$p_k^* = \begin{cases} \bar{P}_k, & \forall k \in \{1, \dots, k^*\}, \\ \frac{\eta^*}{|h_k|^2}, & \forall k \in \{k^* + 1, \dots, K\}, \end{cases} \quad (40)$$

where the threshold is given as

$$\eta^* = \tilde{\eta}_{k^*} = \left(\frac{\sigma^2 + \sum_{i=1}^{k^*} \bar{P}_i |h_i|^2}{\sum_{i=1}^{k^*} \sqrt{\bar{P}_i} |h_i|} \right)^2. \quad (41)$$

Furthermore, it holds that $\bar{P}_k|h_k|^2 \leq \eta^*$ for devices $k \in \{1, \dots, k^*\}$ and $\bar{P}_k|h_k|^2 \geq \eta^*$ for devices $k \in \{k^* + 1, \dots, K\}$. The optimal power-control policy over devices has a *threshold-based structure*. The threshold is specified by the denoising factor η^* and applied on the derived quality indicator $\bar{P}_k|h_k|^2$ accounting for both the channel power gain and power budget of device $k \in \mathcal{K}$. It is shown that for each device $k \in \{k^* + 1, \dots, K\}$ with its quality indicator exceeding the threshold, i.e., $\bar{P}_k|h_k|^2 \geq \eta^*$, the *channel-inversion power control* is applied with $p_k^* = \frac{\eta^*}{|h_k|^2}$; while for each device $k \in \{1, \dots, k^*\}$ with $\bar{P}_k|h_k|^2 \leq \eta^*$, the *full power transmission* is deployed with $p_k^* = \bar{P}_k$.

2) *MIMO AirComp*: In a communication system equipped with antenna arrays, spatial multiplexing enables simultaneous transmission of parallel data streams without requiring additional bandwidth. In the context of AirComp, spatial multiplexing can be leveraged to enhance computational throughput or support vector-function computation, with the multiplexing gain linearly increasing with antenna sizes.

The result is termed MIMO AirComp. Some spatial degrees-of-freedom (DoF) can be also allocated to minimizing the AirComp error by exploiting spatial diversity.

In a single-antenna system, the conventional technique for scalar-function AirComp is relatively simple as it mostly involves channel inversion at each transmitter (e.g., sensor). The techniques for MIMO AirComp is sophisticated. While channel inversion remains optimal as implemented as zero-forcing beamforming, the optimization of receive beamforming, called aggregation beamforming, has been found to be NP-hard, as shown in the sequel. A standard approach can be applied to solve the problem based on *semidefinite programming* (SDP) to design an efficient iterative interior point algorithm. But little insight can be derived. Researchers have found a close-to-optimal solution revealing that the optimal aggregation beamforming has the interesting form of a weighted centroid of multiuser MIMO channels projected onto a Grassmann manifold (or simply called a Grassmannian). This will be the focus of our exposition in the remainder of this section.

To formulate the optimization problem for aggregation beamforming, it is necessary to introduce some additional notation. Let $\mathbf{s}_k \in \mathbb{C}^Q$ be a Q -length baseband signal transmitted by user k , and $\mathbf{B}_k \in \mathbb{C}^{N_t \times Q}$ the transmit beamforming matrix at transmitter k . N_t and N_r are the number of transmit and receive antennas, respectively. The signal at the input of the receiver is $\mathbf{y} \in \mathbb{C}^{N_r}$ and the signal model in (1) turns into

$$\mathbf{y} = \sum_{k=1}^K \mathbf{H}_k \mathbf{B}_k \mathbf{s}_k + \mathbf{n}, \quad (42)$$

where $\mathbf{H}_k \in \mathbb{C}^{N_r \times N_t}$ represents the MIMO channel matrix for the link from the transmitter k to the receiver, and \mathbf{n} is noise vector distributed as $\mathcal{CN}(0, \sigma_n^2)$ elements.

The ultimate goal of the AirComp MIMO scheme is not to recover each individual \mathbf{s}_k , but the sum $\sum_{k=1}^K \mathbf{s}_k$. For this reason, the received signal is further processed with a receive beamforming matrix $\mathbf{A} \in \mathbb{C}^{N_r \times Q}$:

$$\hat{\mathbf{s}} = \mathbf{A}^H \mathbf{y} = \mathbf{A}^H \sum_{k=1}^K \mathbf{H}_k \mathbf{B}_k \mathbf{s}_k + \mathbf{A}^H \mathbf{n}, \quad (43)$$

We define the desired function as $\mathbf{f} = \sum_k \mathbf{s}_k$ and its noisy version $\hat{\mathbf{f}} = \sum_k \hat{\mathbf{s}}_k$. Then the AirComp error is defined by the following MSE:

$$\text{MSE}(\hat{\mathbf{f}}, \mathbf{f}) = \mathbb{E} \left[\|\mathbf{f} - \hat{\mathbf{f}}\|^2 \right] = \mathbb{E} \left[\text{tr} \left(\sum_k \mathbf{s}_k - \sum_k \hat{\mathbf{s}}_k \right) \left(\sum_k \mathbf{s}_k - \sum_k \hat{\mathbf{s}}_k \right)^H \right]. \quad (44)$$

Substituting (43) into (44), the MSE can be explicitly written as a function of the transmit and receive

beamformer as follows:

$$\text{MSE}(\mathbf{A}, \{\mathbf{B}_k\}) = \sum_{k=1}^K \text{tr} \left((\mathbf{A}^H \mathbf{H}_k \mathbf{B}_k - \mathbf{I})(\mathbf{A}^H \mathbf{H}_k \mathbf{B}_k - \mathbf{I})^H \right) + \sigma_n^2 \text{tr}(\mathbf{A}^H \mathbf{A}). \quad (45)$$

Consider the joint optimization of the transmit and aggregation beamformers to minimize the MSE. As transmitters are typically sensors with limited power, it is necessary to set a constraint on average transmission power of each transmitter such that $\|\mathbf{B}_k\|^2 \leq P_0$ for all k with $k = 1, 2, \dots, K$. Following a common approach in the MIMO beamforming literature, the receive beamformer \mathbf{A} is constrained to be orthonormal matrix. Moreover, under the MMSE (i.e., minimum AirComp error) criterion, the denoising factor (positive scalar) can be absorbed into \mathbf{A} for regulating the tradeoff between noise reduction and transmission-power control. We can write $\mathbf{A} = \sqrt{\eta} \mathbf{F}$ with \mathbf{F} being a tall unitary matrix and thus $\mathbf{F}^H \mathbf{F} = \mathbf{I}$. Then given the AirComp error in (45), the aggregation beamforming problem can be formulated as:

$$\begin{aligned} & \min_{\eta, \mathbf{A}, \{\mathbf{B}_k\}} \text{MSE}(\mathbf{A}, \{\mathbf{B}_k\}) \\ (\mathbf{P2}) \quad & \text{s.t. } \|\mathbf{B}_k\|^2 \leq P_0, \quad \forall k, \\ & \mathbf{A}^H \mathbf{A} = \eta \mathbf{I}. \end{aligned}$$

Problem (P2) is difficult to solve due to its non-convexity. The lack of convexity arises from the coupling between transmit and receive beamformers in the objective function, and the orthogonality constraint on the receive beamformer. It can be proved that zero-forcing transmit beamforming conditioned on an aggregation beamformer as given below is optimal as follows [39]

$$\mathbf{B}_k^* = (\mathbf{A}^H \mathbf{H}_k)^H (\mathbf{A}^H \mathbf{H}_k \mathbf{H}_k^H \mathbf{A})^{-1}, \quad \forall k. \quad (46)$$

As a result, Problem (P2) is transformed to the equivalent problem of minimizing the denoising factor of the receive beamformer:

$$\begin{aligned} & \min_{\eta, \mathbf{F}} \eta \\ (\mathbf{P3}) \quad & \text{s.t. } \frac{1}{\eta} \text{tr} \left((\mathbf{F}^H \mathbf{H}_k \mathbf{H}_k^H \mathbf{F})^{-1} \right) \leq P_0, \quad \forall k, \\ & \mathbf{F}^H \mathbf{F} = \mathbf{I}, \end{aligned}$$

where \mathbf{F} is defined earlier as the normalized receive beamformer. To develop a tractable approximation of the problem, we can modify the power constraints with an approximate form. This requires *singular value decomposition* (SVD) of \mathbf{H}_k of each MIMO channel: $\mathbf{H}_k = \mathbf{U}_k \Sigma_k \mathbf{V}_k^H$. As a result, Problem (P3) can be approximated by the following problem with tightened power constraints and invoking differential

geometry theory to reveal its equivalence to the following form that contains subspace distances between the aggregation beamformer and individual MIMO channels (see details in [39])

$$\begin{aligned}
 (\text{P4}) \quad & \max_{\mathbf{F}} \sum_{k=1}^K \lambda_{\min}(\Sigma_k^2) \text{tr}(\mathbf{U}_k^H \mathbf{F} \mathbf{F}^H \mathbf{U}_k) \\
 & \text{s.t. } \mathbf{F}^H \mathbf{F} = \mathbf{I}.
 \end{aligned} \tag{47}$$

$$d_{\text{PF}}^2(\mathbf{U}_k, \mathbf{F}) = N_t - \text{tr}(\mathbf{U}_k^H \mathbf{F} \mathbf{F}^H \mathbf{U}_k).$$

Problem (P4) remains non-convex due to 1) maximizing a convex objective function and 2) the orthogonality constraints on the variable \mathbf{F} . Nevertheless, by intelligently constructing an equivalent unconstrained problem, we are able to derive a closed-form solution via analyzing the stationary points of the unconstrained problem. For ease of exposition, define a matrix $\mathbf{G} \in \mathbb{C}^{N_r \times N_r}$ as follows:

$$\mathbf{G} = \sum_{k=1}^K \lambda_{\min}(\Sigma_k^2) \mathbf{U}_k \mathbf{U}_k^H. \tag{48}$$

Let $\mathbf{G} = \mathbf{V}_G \Sigma_G \mathbf{V}_G^H$ be the SVD of \mathbf{G} given in (48). The solution is given by the first L principal eigen-vectors of \mathbf{G} , namely

$$\mathbf{F}^* = [\mathbf{V}_G]_{:,1:L}. \tag{49}$$

It follows that the optimal aggregation beamforming matrix is given as $\mathbf{A}^* = \sqrt{\eta^*} \mathbf{F}^*$, with \mathbf{F}^* in (49) while the corresponding denoising factor is given as

$$\eta^* = \max_k \frac{1}{P_0} \text{tr}(((\mathbf{F}^*)^H \mathbf{H}_k \mathbf{H}_k^H \mathbf{F}^*)^{-1}). \tag{50}$$

Lets interpret the geometry structure of the above optimal aggregation beamformer. Each unitary matrix in (48), \mathbf{U}_k , represents the spatial orientation of MIMO channel k . \mathbf{U}_k appears as a single point on a Grassmann manifold, which can be interpreted as the space of subspaces. As a result, \mathbf{G} is a weighted sum of MIMO channels projected onto the Grassmann manifold with weights related to the channels eigenvalues (or equivalently their norms). Being a derivative of \mathbf{G} , the aggregation beamformer \mathbf{A}^* allows the same geometric interpretation.

B. Partial CSI: Synchronization impairments

In practice, transmitted signals are exposed to hardware imperfections in addition to the distortions in the propagation medium. While some of these impairments, such as power amplifier non-linearity, can be single-sided, i.e., occurring only at transmitters, the distortions like timing errors due to the imperfect

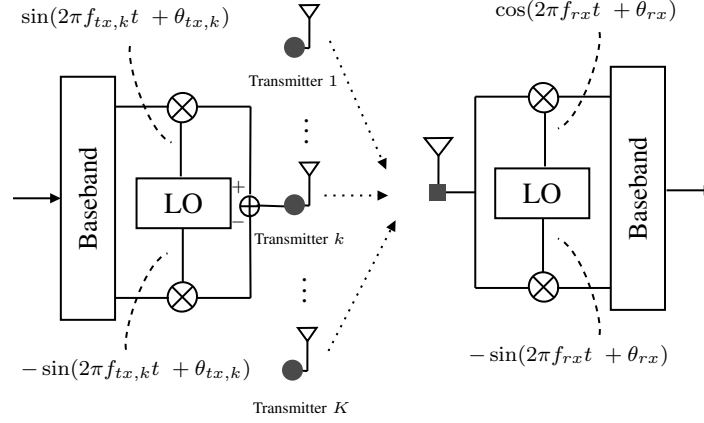


Fig. 10. Hardware imperfections regarding carrier frequency offset and phase offset.

clock feeding the digital circuit, residual synchronization errors in the baseband, carrier frequency offset, phase offset, and phase noise in RF front-end, can occur at both transmitter and receiver. Most of these impairments can be addressed well in communication scenarios as the distortion can be estimated and corrected, particularly at the receiver. However, the same methods used for communications may not be directly applied to computation as the receiver observes the superposed distorted transmitted signals in AirComp, resulting in a new plethora of research topics and new AirComp schemes for reliable computations. Next, we assess the impact of synchronization impairments in AirComp. Unlike in the previous subsection VI-A, the signal processing techniques applied in this section are not constrained to amplitude modulations. Furthermore, we assume $L \geq 1$ and a single antenna per transmitter and receiver.

Let $\{f_{tx,k}, \theta_{tx,k}\}$ and $\{f_{rx}, \theta_{rx}\}$ be the carrier frequency and the phase of the local oscillator (LO) at the k -th transmitter and the receiver, respectively, as shown in Fig. 10, and further completing the formulation of the transmitted passband signals in (26) as

$$x_k^{pb}(t) = \Re\{x_k(t)e^{j2\pi f_{tx,k}t + j\theta_{tx,k}}\}. \quad (51)$$

The received passband signal for the k -th transmitter can then be expressed as

$$r_k^{pb}(t) = h_k(t) \otimes x_k^{pb}(t) = \Re\left\{e^{j2\pi f_{rx}t + j\theta_{rx}} \underbrace{\sum_{p=1}^P h_{k,p} e^{j\Delta\theta_k} x_k(t - \tau_{k,p}) e^{j2\pi\Delta f_k(t - \tau_{k,p})}}_{\triangleq r_k(t)}\right\} \quad (52)$$

where $\Delta f_k \triangleq f_{tx,k} - f_{rx}$, and $\Delta\theta_k \triangleq \theta_{tx,k} - \theta_{rx}$ and the carrier frequency offset (CFO) and the phase offset (PO) between the k th transmitter and the receiver, respectively, and $r_k(t)$ is the received complex

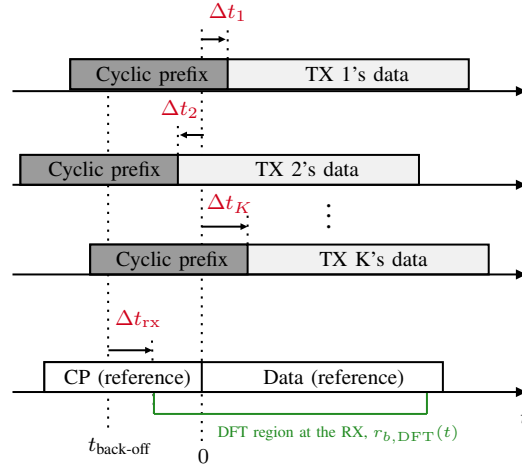


Fig. 11. Time synchronization errors at the transmitter and receivers. The receiver backs off by $t_{\text{back-off}}$ seconds for the DFT window to avoid samples from the subsequent OFDM symbol in practice while it can still be out-of-sync by Δt_{rx} second like the transmitters.

baseband signal for $h_{k,p}(t) \triangleq h_{k,p}^c e^{-j2\pi f_{\text{rx}} \tau_{k,p}}$.

Now, suppose that the following conditions hold for all transmitters:

- Condition 1: $\Delta\theta_k$ is not a function of time. Condition 1 implies that the transmitters and receiver do not power down their LOs at any time. It also requires very accurate crystals; otherwise, $\Delta\theta_k$ becomes random.
- Condition 2: The *baseband* signal $x_k(t)$ is offset by $\Delta t_{\text{tx},k}$ relative to the receiver's synchronization point $t_{\text{back-off}}$ and offsets are not jittery. Condition 2 does not consider potential jitters in the passband signal, which can lead to an additional phase rotation that is very sensitive to the value of carrier frequency.
- Condition 3: Frequency synchronization is ideal, i.e., $\Delta f_k = 0$. If Condition 3 is violated (e.g., residual CFO after correction), phase error accumulation over time occurs, as seen from (52). Hence, coherent AirComp can be very sensitive to channel aging.

Considering the widespread adoption of OFDM in wireless networks, its robustness against multipath channels, and its compatibility with a wide range of waveforms via transform precoders (e.g., DFT-precoder for a single-carrier waveform), suppose that symbols for AirComp are transmitted with an orthogonal frequency division multiplexing (OFDM) symbol of duration T_{sym} as

$$x_k(t) = \begin{cases} \sum_{l=0}^{Q-1} a_{kl} e^{j2\pi l \frac{t - \Delta t_{\text{tx},k}}{T_{\text{sym}}}}, & -T_{\text{cp}} + \Delta t_{\text{tx},k} \leq t < T_{\text{sym}} + \Delta t_{\text{tx},k} \\ 0, & \text{otherwise} \end{cases}, \quad (53)$$

Under Conditions 1-3, we can then express the superposed waveform for $t \in [t_{\text{back-off}}, T_{\text{sym}} - t_{\text{back-off}})$, i.e., the DFT processing window at the receiver as shown in Fig. 11, as

$$r(t) = \sum_{l=0}^{Q-1} \underbrace{\sum_{k=1}^K H_{k,l} e^{j\Delta\theta_k} e^{j2\pi l \frac{t_{\text{back-off}} - \Delta t_{\text{rx}} - \Delta t_{\text{tx},k}}{T_{\text{sym}}}}}_{\text{superposed symbols in the frequency domain}} a_{k,l} e^{j2\pi l \frac{t}{T_{\text{sym}}}}, \quad (54)$$

for $H_{k,l} \triangleq \sum_{p=1}^P h_{k,p}^c e^{j2\pi l \frac{\tau_{k,p}}{T_{\text{sym}}}}$, i.e., the frequency response of the multipath channel. We can now infer the following results:

- Under Conditions 1-3, the phase term in (54) due to the offsets increases with the subcarrier index ℓ for $t_{\text{back-off}} - \Delta t_{\text{rx}} - \Delta t_{\text{tx},k} \neq 0$.
- Equation (54) shed light on AirComp based on single-carrier waveform. The phase term in (54) due to the time misalignment is zero for the DC subcarrier, i.e., $\ell = 0$, which corresponds to a single carrier waveform with a rectangular pulse.
- The main issue for coherent AirComp is not time offset (TO) or PO themselves, but the jitters on TO or PO under Conditions 1-3. This is because a channel estimator estimates the composite response of the channel, i.e., $H_{k,l} e^{j\Delta\theta_k} e^{j2\pi l \frac{t_{\text{back-off}} - \Delta t_{\text{rx}} - \Delta t_{\text{tx},k}}{T_{\text{sym}}}}$, rather than the solely multi-path channel. Hence, it is crucial to keep the POs and TOs as fixed as possible for coherent AirComp.

Conditions 1-3 introduce stringent design constraints for practical wireless networks. Hence, a fundamental challenge is how to achieve AirComp without relying on the availability of phase synchronization in the network or the availability of instantaneous CSI at the nodes, leading to various non-coherent approaches. One of the key ideas exploited in literature is to dedicate different resources representing a set of classes and use the energy accumulation on these resources to obtain an approximate histogram, i.e., TBMA, discussed in Section III. For example, in a binary format, two classes may defined as 0 and 1, and a non-coherent AirComp can encode the binary information for each digit and the sum of digits can be exploited as discussed in Section VI.1.b.

Another key idea is to modulate the norm-square of the sequence with the magnitude of the parameter, proposed in [20]. This approach is different from the aforementioned TBMA-based non-coherent approaches in that it achieves continuous-valued aggregation while still exploiting the energy accumulation in the medium. In this approach, the output of the pre-processing function is processed further with a function g that results in a non-negative value. Subsequently, the *square root* of the resulting value is multiplied with a sequence of length Q as $\sqrt{g(s_k)} \times [e^{j\theta_1}, \dots, e^{j\theta_Q}]$, i.e., the norm-square of the sequence linearly changes with $g(s_k)$. At the receiver, the energy of the received sequence is calculated to achieve the AirComp, and the superposed symbol is processed with another affine function h to reverse the impact

of g on the superposed symbols. It is worthwhile noting that the affine function at the receiver is a function of the number of transmitters participating in the computation. As the receiver calculates the energy of the received sequence with this technique, the scheme is not sensitive to phase synchronization errors. However, the price paid is the cross-product terms due to the loss of orthogonality of the sequences in an overcomplete space for AirComp with limited resources. In [20], unimodular sequences with random phases are adopted to reduce the cross-product terms, but it is emphasized that the design of the sequence should harness interference as a common goal instead of eliminating the interference as in a traditional code division multiple access systems. Currently, the optimal sequence set for Goldenbaum's approach is an open question.

VII. SECURITY IN AIRCOMP

AirComp relies on the superposition of the transmitted signals. Hence, it has both positive and negative implications regarding security. On the one hand, the superposition in AirComp promotes user privacy as the transmitted signals cannot be directly observed. On the other hand, it opens up potential adversaries to harm the computation, and their impact cannot be directly inferred [5], [6]. The security aspects of AirComp may be investigated in four categories: Byzantine attacks, jamming, privacy, and eavesdropping.

Byzantine attacks are launched by the adversary or faulty nodes already part of the network, and AirComp is sensitive to these attacks. For example, for FEEL with AirComp, if the local data at the nodes are deliberately labeled incorrect (i.e., one of the data poisoning attacks) or the sign of the gradients are flipped (i.e., one of the model poisoning attacks) and the aggregation is handled through an AirComp scheme, the learning process can be unreliable. For AirComp, a Byzantine attack is a major problem because well-known precaution strategies relying on the observation of local information cannot be utilized directly as the computing node observes the superposed signal, not the signals transmitted themselves [40]. To improve resilience against such attacks, several authors investigate the Weiszfeld algorithm and implement the corresponding iterations steps by considering AirComp, which is also in line with computing the median function or majority vote [41]. Another strategy is that the network divides the nodes into multiple groups in orthogonal resources, uses AirComp for each group, and compares the distances among the groups [42]. Like Byzantine attacks, AirComp can be sensitive to jamming. Compared to the Byzantine attackers, jammers are not part of the network. Hence, it can be easier to detect the presence of jammers. One advantage of AirComp is that it is inherently distributed and can provide resilience against jammers, provided that the jamming signal is less powerful than the superposed signal. One way to improve resilience against jammers further is to use a common spreading code, assuming that

the jammers do not know the spreading code. Hence, the interference due to the adversary is suppressed in the de-spreading operation at the computing node [19].

AirComp promotes privacy as the local information is not observed. Also, it can accommodate existing privacy-enhancing methods. For example, a typical approach is to randomize the disclosed statistics by adding random or artificial noise, which causes a trade-off between accuracy and privacy [43]. For example, for FEEL, these random perturbations can be added to the model parameters or gradients before signal superposition to enhance privacy. Since AirComp can also be used with channel inversion at the transmitters, arguably, privacy can be promoted further [44].

AirComp can be sensitive to eavesdropping depending on the AirComp scheme. If the AirComp uses channel state information at the transmitters, an eavesdropper cannot directly observe the coherently superposed signal, and it provides a level of physical layer security against eavesdroppers. However, if AirComp relies on non-coherent computations for robust computation or does not rely on channels at the transmitters to address hardware impairments, it becomes vulnerable to eavesdropping. To address this issue, one approach is to divide the transmitter into two groups based on the amplitude of the channels and use a group of nodes with weaker channel conditions as jammers [45]. Another method is to inject artificial noise at the computing node, where the computing node removes the noise from the signal superposition [46]. Also, homomorphic encryption methods can be used along with AirComp as they allow superposed symbols to be encrypted without the secret key [47].

VIII. CONCLUSIONS AND FUTURE RESEARCH

Future communication systems will focus on enabling higher-level tasks rather than merely transmitting data, necessitating redesigns to meet specific application or computational requirements. Reducing computational complexity and delays may become more critical than minimizing bit error rates. In this context, AirComp presents a highly attractive alternative. This article highlights the challenge AirComp poses for signal processing and waveform design in radio transmission. A systematic review of the different alternatives in the literature, together with the design guidelines to face the communication channel, are presented in this paper.

The modulation sections expand the range of possible waveforms to include not only amplitude but also angular modulations, thanks to TBMA. Note that angular modulations are more attractive than amplitude ones due to their robustness against channel attenuation, as the information is not encoded in the waveform's amplitude. A general approach to the joint optimization of pre-processing, waveform, and post-processing is also formulated in (21). One can think of future neural networks to address this complex joint optimization problem, where MSE or other of the metrics that have been introduced in

section II-C can be used according to the final application purposes. Note that these neural networks should consider the constraints imposed by the specific computation and application. These constraints are on: power, transmission bandwidth, number of nodes, quantization error, and maximum calculation error allowed. The complexity supported by the transmitting nodes must also be considered in this optimization. For example, due to the continuous demand for higher bandwidth in IoT networks (e.g., an increased number of interconnected entities or multimedia sensors for surveillance), binary minimum shift keying (MSK) or differential modulations (e.g., differential pulse code modulation (PCM)) become appealing. They modulate the difference between successive samples rather than the sample itself, which helps reduce traffic with event-based sampling by selectively transmitting significant differences based on the application, resulting in an effective sampling rate below the Nyquist rate [22]. Developing AirComp schemes for these IoT modulation schemes is an open area of research.

Additionally, integrating compressed sensing, as discussed in [16], in the pre-processing stage presents an interesting challenge. With the increasing development of AI systems and semantic communications, source encoders are expected to extract high-level features from data, providing gains similar to how traditional voice communication systems extract spectral content from voice data conveyed through the channel [48].

Another critical aspect is designing the physical layer frame to introduce the most suitable multiplexing and/or diversity techniques based on the wireless channel and implementation constraints. To date, OFDM has emerged as the best solution for solving time synchronization problems between different transmitters and handling channels with frequency-selective fading. However, other non-multicarrier options may be more interesting when bandwidth is limited, as for instance, the MIMO techniques that we revisit in this paper. Note, however, that the existing signal processing techniques for AirComp are mainly developed for DA, but not in the context of TBMA. Overall, many existing signal processing techniques designed to enhance the diversity or multiplexing capabilities of point-to-point or non-AirComp MAC systems can potentially be adapted and applied to AirComp. This opens up a whole range of problems within signal processing.

Finally, the design of channel codes for AirComp is an open research topic. AirComp requires new channel codes that comply with the additive nature of the scheme, meaning the addition of redundancy must provide useful information at the receiver [24]. Some ideas may be borrowed from coded computing [49], which aims to overcome fundamental bottlenecks in wireless systems with massive numbers of distributed computing nodes, such as communication complexity and latency. As several challenges remain unresolved when underlying codes are designed over discrete spaces (e.g., overflow errors), analog error-correcting codes are suitable for applications, such as learning, that are insensitive to controlled

inaccuracies. Methods and ideas for optimal codes over discrete spaces cannot be extended to continuous spaces due to fundamental differences. These issues have motivated researchers to rethink code design over continuous spaces for specific applications where data is inherently real/complex-valued [50]. AirComp can benefit from and follow these new coding trends, presenting a green field for exploration with signal processing.

REFERENCES

- [1] M. Goldenbaum, H. Boche, and S. Stanczak, "Harnessing interference for analog function computation in wireless sensor networks," *IEEE Transactions on Signal Processing*, vol. 61, no. 20, pp. 4893–4906, 2013.
- [2] B. Nazer and M. Gastpar, "Computation over multiple-access channels," *IEEE Transactions on Information Theory*, vol. 53, no. 10, pp. 3498–3516, 2007.
- [3] M. Gastpar, M. Vetterli, and P. Dragotti, "Sensing reality and communicating bits: a dangerous liaison," *IEEE Signal Processing Magazine*, vol. 23, no. 4, pp. 70–83, 2006.
- [4] D. Gunduz, Z. Qin, I. Estella, H. S. Dhillon, Z. Yang, A. Yener, K. K. Wong, and C.-B. Chae, "Beyond transmitting bits: Context, semantics, and task-oriented communications," *IEEE Journal on Selected Areas in Communications*, vol. 41, no. 1, pp. 5–41, 2023.
- [5] H. Hellström, J. M. B. da Silva Jr., M. M. Amiri, M. Chen, V. Fodor, H. V. Poor, and C. Fischione, *Wireless for Machine Learning: A Survey*. Foundations and Trends in Signal Processing, 2022, vol. 15, no. 4.
- [6] A. Şahin and R. Yang, "A survey on over-the-air computation," *IEEE Communications Surveys & Tutorials*, vol. 25, no. 3, pp. 1877–1908, 2023.
- [7] Z. Wang, Y. Zhao, Y. Zhou, Y. Shi, C. Jiang, and K. B. Letaief, "Over-the-air computation: Foundations, technologies, and applications," *arXiv preprint arXiv:2210.10524*, 2022.
- [8] M. Dohler, R. Heath, A. Lozano, C. Papadias, and R. Valenzuela, "Is the phy layer dead?" *IEEE Communications Magazine*, vol. 49, no. 4, pp. 159–165, 2011.
- [9] C.-T. Chu, S. Kim, Y.-A. Lin, Y. Yu, G. Bradschi, K. Olukotun, and A. Ng, "Map-reduce for machine learning on multicore," *Advances in neural information processing systems*, vol. 19, pp. 281–288, 2006.
- [10] X. Wu, S. Zhang, and A. Ozgur, "Stac: Simultaneous transmitting and air computing in wireless data center networks," *IEEE Journal on Selected Areas in Communications*, vol. 34, no. 12, pp. 4024–4034, 2016.
- [11] B. Song, C. Ding, A. T. Kamal, J. A. Farrell, and A. K. Roy-chowdhury, "Distributed camera networks," *IEEE Signal Processing Magazine*, vol. 28, no. 3, pp. 20–31, 2011.
- [12] Z. Liu, Q. Lan, A. E. Kalr, P. Popovski, and K. Huang, "Over-the-air view-pooling for low-latency distributed sensing," in *2023 IEEE 24th International Workshop on Signal Processing Advances in Wireless Communications (SPAWC)*, 2023, pp. 71–75.
- [13] J. Lee, Y. Jang, H. Kim, S.-L. Kim, and S.-W. Ko, "Over-the-air consensus for distributed vehicle platooning control," in *ICC 2023 - IEEE International Conference on Communications*, 2023, pp. 5965–5971.
- [14] A. Şahin, "Wireless federated k -means clustering with non-coherent over-the-air computation," in *Proc. IEEE Military Communications Conference (MILCOM)*, 2023, pp. 339–344.
- [15] R. Guirado, A. Rahimi, G. Karunaratne, E. Alarcon, A. Sebastian, and S. Abadal, "Whype: A scale-out architecture with wireless over-the-air majority for scalable in-memory hyperdimensional computing," *IEEE Journal on Emerging and Selected Topics in Circuits and Systems*, vol. 13, no. 1, pp. 137–149, 2023.

- [16] J.-J. Xiao, S. Cui, Z.-Q. Luo, and A. J. Goldsmith, "Linear coherent decentralized estimation," *IEEE Transactions on Signal Processing*, vol. 56, no. 2, pp. 757–770, 2008.
- [17] M. Goldenbaum, H. Boche, and S. Stanczak, "Nomographic functions: Efficient computation in clustered gaussian sensor networks," *IEEE Transactions on Wireless Communications*, vol. 14, no. 4, pp. 2093–2105, 2015.
- [18] M. Martínez-Gost, A. Pérez-Neira, and M. Á. Lagunas, "ENN: A neural network with DCT-adaptive activation functions," *IEEE Journal of Selected Topics in Signal Processing*, 2023.
- [19] G. Zhu, Y. Wang, and K. Huang, "Broadband analog aggregation for low-latency federated edge learning," *IEEE Transactions on Wireless Communications*, vol. 19, no. 1, pp. 491–506, 2020.
- [20] M. Goldenbaum and S. Stanczak, "Robust analog function computation via wireless multiple-access channels," *IEEE Transactions on Communications*, vol. 61, no. 9, pp. 3863–3877, 2013.
- [21] X. Cao, G. Zhu, J. Xu, and K. Huang, "Optimized power control for over-the-air computation in fading channels," *IEEE Transactions on Wireless Communications*, vol. 19, no. 11, pp. 7498–7513, 2020.
- [22] U. Premaratne, S. Warnakulasooriya, and R. Nandana, "Characterization of event-based sampling encoders for industrial internet of things using inputoutput mutual information," *IEEE Transactions on Industrial Informatics*, vol. 17, no. 8, pp. 5495–5505, 2021.
- [23] A. B. Carlson and P. Crilly, *Communication systems*. McGraw-Hill Education, 2009.
- [24] X. Xie, C. Hua, J. Hong, and Y. Wei, "Joint design of coding and modulation for digital over-the-air computation," *arXiv preprint arXiv:2311.06829*, 2023.
- [25] G. Mergen and L. Tong, "Type based estimation over multiaccess channels," *IEEE Transactions on Signal Processing*, vol. 54, no. 2, pp. 613–626, 2006.
- [26] M. Martínez-Gost, A. Prez-Neira, and M. Á. Lagunas, "LoRa-based over-the-air computing for Sat-IoT," in *2023 31st European Signal Processing Conference (EUSIPCO)*, 2023, pp. 1514–1518.
- [27] A. Şahin, "Over-the-air computation based on balanced number systems for federated edge learning," *IEEE Transactions on Wireless Communications*, vol. 23, no. 5, pp. 4564–4579, 2024.
- [28] M. Martínez-Gost, A. Pérez-Neira, and M. Á. Lagunas, "Log-FSK: A frequency modulation for over-the-air computing," *EUSIPCO*, 2024.
- [29] M. M. Gost, A. Prez-Neira, and M. Á. Lagunas, "DCT-based air interface design for function computation," *IEEE Open Journal of Signal Processing*, vol. 4, pp. 44–51, 2023.
- [30] R. Guirado, A. Rahimi, G. Karunaratne, E. Alarcón, A. Sebastian, and S. Abadal, "Whype: A scale-out architecture with wireless over-the-air majority for scalable in-memory hyperdimensional computing," *IEEE Journal on Emerging and Selected Topics in Circuits and Systems*, vol. 13, no. 1, pp. 137–149, 2023.
- [31] S. Razavikia, J. M. B. Da Silva, and C. Fischione, "Channelcomp: A general method for computation by communications," *IEEE Transactions on Communications*, pp. 1–1, 2023.
- [32] N. Sidiropoulos, T. Davidson, and Z.-Q. Luo, "Transmit beamforming for physical-layer multicasting," *IEEE Transaction on Signal Processing*, vol. 54, no. 6, pp. 2239–2251, 2006.
- [33] L. Vandenberghe and S. Boyd, "Semidefinite programming," *SIAM review*, vol. 38, no. 1, pp. 49–95, 1996.
- [34] Z.-Q. Luo, W.-K. Ma, A. M.-C. So, Y. Ye, and S. Zhang, "Semidefinite relaxation of quadratic optimization problems," *IEEE Signal Processing Magazine*, vol. 27, no. 3, pp. 20–34, 2010.
- [35] S. Razavikia, J. M. B. D. S. Jnior, and C. Fischione, "Sumcomp: Coding for digital over-the-air computation via the ring of integers," 2023.

- [36] A. Şahin, “Distributed learning over a wireless network with non-coherent majority vote computation,” *IEEE Transactions on Wireless Communications*, vol. 22, no. 11, pp. 8020–8034, 2023.
- [37] M. Martinez-Gost, A. Perez-Neira, and M. . Lagunas, “Frequency modulation aggregation for federated learning,” in *GLOBECOM 2023 - 2023 IEEE Global Communications Conference*, 2023, pp. 1878–1883.
- [38] G. Zhu, Y. Du, D. Gunduz, and K. Huang, “One-bit over-the-air aggregation for communication-efficient federated edge learning: Design and convergence analysis,” *IEEE Transactions on Wireless Communications*, vol. 20, no. 3, pp. 2120–2135, 2021.
- [39] G. Zhu and K. Huang, “Mimo over-the-air computation for high-mobility multimodal sensing,” *IEEE Internet of Things Journal*, vol. 6, no. 4, pp. 6089–6103, 2019.
- [40] X. Fan, Y. Wang, Y. Huo, and Z. Tian, “BEV-SGD: Best effort voting SGD against byzantine attacks for analog aggregation based federated learning over the air,” *IEEE Internet of Things Journal*, pp. 1–14, 2022.
- [41] S. Huang, Y. Zhou, T. Wang, and Y. Shi, “Byzantine-resilient federated machine learning via over-the-air computation,” in *Proc. IEEE International Conference on Communications Workshops (ICC Workshops)*, 2021, pp. 1–6.
- [42] S. Park and W. Choi, “Byzantine fault tolerant distributed stochastic gradient descent based on over-the-air computation,” *IEEE Trans. Commun.*, pp. 1–15, 2022.
- [43] M. Seif, R. Tandon, and M. Li, “Wireless federated learning with local differential privacy,” in *Proc. IEEE International Symposium on Information Theory (ISIT)*, 2020, pp. 2604–2609.
- [44] D. Liu and O. Simeone, “Privacy for free: Wireless federated learning via uncoded transmission with adaptive power control,” *IEEE Journal on Selected Areas in Communications*, vol. 39, no. 1, pp. 170–185, 2021.
- [45] H. Jeon, D. Hwang, J. Choi, H. Lee, and J. Ha, “Secure type-based multiple access,” *IEEE Transactions on Information Forensics and Security*, vol. 6, no. 3, pp. 763–774, 2011.
- [46] M. Frey, I. Bjelakovic, and S. Stanczak, “Towards secure over-the-air computation,” in *Proc. IEEE International Symposium on Information Theory (ISIT)*, 2021, pp. 700–705.
- [47] R.-A. Stoica, O. Taghizadeh, and S. B. Mary Baskaran, “Secret computing over multiple access channels,” in *2022 56th Asilomar Conference on Signals, Systems, and Computers*, 2022, pp. 559–563.
- [48] Y. Blau and T. Michaeli, “The perception-distortion tradeoff,” in *Proceedings of the IEEE conference on computer vision and pattern recognition*, 2018, pp. 6228–6237.
- [49] S. Li and S. Avestimehr, “Coded computing: Mitigating fundamental bottlenecks in large-scale distributed computing and machine learning,” *Foundations and Trends in Communications and Information Theory*, vol. 17, no. 1, pp. 1–148, 2020.
- [50] M. Soleymani, “Analog coding: Theory and applications,” PhD thesis, University of Michigan, Michigan, MI, 2022.